REPRESENTING SUDDEN SHIFTS IN INTENSIVE DYADIC INTERACTION DATA USING DIFFERENTIAL EQUATION MODELS WITH REGIME SWITCHING

SY-MIIN CHOW AND LU OU

PENNSYLVANIA STATE UNIVERSITY

ARRIDHANA CIPTADI

GEORGIA INSTITUTE OF TECHNOLOGY

EMILY B. PRINCE

UNIVERSITY OF MIAMI

DONGJUN YOU

PENNSYLVANIA STATE UNIVERSITY

MICHAEL D. HUNTER

UNIVERSITY OF OKLAHOMA HEALTH SCIENCES CENTER

JAMES M. REHG AND AGATA ROZGA

GEORGIA INSTITUTE OF TECHNOLOGY

DANIEL S. MESSINGER

UNIVERSITY OF MIAMI

A growing number of social scientists have turned to differential equations as a tool for capturing the dynamic interdependence among a system of variables. Current tools for fitting differential equation models do not provide a straightforward mechanism for diagnosing evidence for qualitative shifts in dynamics, nor do they provide ways of identifying the timing and possible determinants of such shifts. In this paper, we discuss regime-switching differential equation models, a novel modeling framework for representing abrupt changes in a system of differential equation models. Estimation was performed by combining the Kim filter (Kim and Nelson State-space models with regime switching: classical and Gibbs-sampling approaches with applications, MIT Press, Cambridge, 1999) and a numerical differential equation solver that can handle both ordinary and stochastic differential equations. The proposed approach was motivated by the need to represent discrete shifts in the movement dynamics of $n = 29$ mother–infant dyads during the Strange Situation Procedure (SSP), a behavioral assessment where the infant is separated from and reunited with the mother twice. We illustrate the utility of a novel regime-switching differential equation model in representing children's tendency to exhibit shifts between the goal of staying close to their mothers and intermittent interest in moving away from their mothers to explore the room during the SSP. Results from empirical model fitting were supplemented with a Monte Carlo simulation study to evaluate the use of information criterion measures to diagnose sudden shifts in dynamics.

Correspondence should be made to Sy-Miin Chow, Pennsylvania State University, 413 Biobehavioral Health Building, University Park, PA 16802, USA. Email: symiin@psu.edu

Published online: 19 March 2018

Differential equation (DE) models have been one of the most dominant tools for representing change phenomena in disciplines such as the physical sciences, econometrics, engineering, and ecology. In parallel, the statistical and engineering literature has evidenced tremendous growth in methodologies for fitting DE models (Jones 1993; Mbalawata et al., 2013; Beskos et al., 2009; Kulikov & Kulikova, 2014; Kulikova & Kulikov, 2014; Ramsay et al., 2007; Särkkä, 2013). Although uptake in the social and behavioral sciences has been slow, some notable advances have been made in fitting linear ordinary and stochastic differential equation (ODE and SDE, respectively) models using approaches such as exact discrete time (Oud and Jansen, 2000; Oud & Singer, 2008; Singer, 2010, 2012; Voelkle et al., 2012), structural equation modeling (Boker et al., 2008), Bayesian (Oravecz et al., 2011), and two-stage derivative estimation/modeling approaches (Boker and Graham, 1998; Boker et al., 2010; Deboeck, 2010; Chow et al., 2016a; Trail et al., 2013). Developments in fitting nonlinear DEs and those that evidence discontinuities in dynamics are still nascent (e.g., Singer, 2002, 2003; Chow et al., 2007; 2016b; Lu et al., 2015), but have begun to garner some support in modeling particular empirical phenomena (Chow and Zhang, 2013; Chow et al., 2016a; Molenaar & Newell, 2003).

In the present article, we propose adding to the repertoire of dynamic modeling tools a class of models termed *regime-switching differential equation* (RS-DE) models. These models represent change processes that undergo discontinuous changes through distinct, categorical phases, but are otherwise characterized by continuous dynamics within each phase that can be represented by means of a set of linear or nonlinear ODEs/SDEs. ODEs can be viewed as special cases of SDEs wherein the dynamic processes of interest evolve over time in completely deterministic (predictable) ways—namely as exempt from the influence of process noises—provided that complete knowledge of the system is known. The phase or "regime" that governs the nature of the operating DEs is unobserved, but is allowed to vary as contingent on a series of person- (or dyad-, family-) specific and time-varying covariates of interest.

The proposed approach was motivated by the need to represent discrete shifts in the movement dynamics of $n = 29$ mother–infant dyads during the Strange Situation Procedure (SSP), a behavioral assessment where the infant is separated from and reunited with the mother twice. Attachment theory posits that attachment security provides a secure physical and psychological basis for exploration of the environment (Bowlby, 1973, 1982). Thus, during the SSP, most secure children are expected to manifest shifts between a desire to stay close to their caregivers (e.g., mothers), and intermittent interest in moving away from their caregivers to explore the room. Moreover, even though mothers' interactive behaviors with their infants during the SSP play a central role in influencing the infants' subsequent behavior (Behrens et al., 2011), previous studies have rarely analyzed mothers' interactive dynamics with their children as a dynamic and interdependent system. Our motivating problem thus requires the development and estimation of a multivariate DE model that can describe the interactive dynamics between mothers and their children during the SSP, while allowing for sufficient flexibility for some but not all dyads to show intermittent shifts in their interactive dynamics.

The discrete shifts in the children's behavior observed during the SSP are not unlike properties of systems that undergo stagewise changes (e.g., Piaget & Inhelder, 1969; van der Maas & Molenaar, 1992, Fukuda & Ishihara,1997; Van Geert, 2000). However, unlike stagewise theories which posit a unidirectional or *irreversible* progression through a sequence of stages, the transition across phases is reversible and individuals are allowed to switch between regimes over time (Hamilton, 1989; Kim & Nelson, 1999). The operating regime at any particular time point is unknown but can be estimated from the data; the operating regime may also vary across individuals and over time, thus giving rise to intra- and interindividual differences in dynamics. In this

sense, the role of regimes as a latent determinant of systematic individual differences is similar to the role of latent classes in mixture models, except that individuals can transition across different regimes over time; in other words, class membership may change over time (Dolan, 2009). In light of this, we use the terms regime and class interchangeably throughout the paper.

The proposed RS-DE framework extends the work of Chow and Zhang (2013) from a discrete time to a continuous-time framework and is characterized by several unique advantages. First, in contrast to standard linear regime-switching state-space (Kim & Nelson, 1999) models and linear covariance structure models with regime-switching properties (Dolan et al., 2005; Dolan, 2009; Schmittmann et al., 2005), we capitalize on the use of numerical solvers of differential equations to allow the change processes within each regime to evolve in continuous time as linear and/or nonlinear functions of the latent variables and other covariates in the system. Continuous-time functions provide renewed ways of portraying the ongoing interdependencies between multivariate processes at any particular time point, and they have been shown to be useful in representing myriad empirical phenomena elsewhere (Chow et al., 2007, 2016a, 2016b; Lu et al., 2015; Oravecz et al., 2009; Oud & Jansen, 2000; Voelkle et al., 2012). Second, aside from their theoretical appeal, DEs also offer several practical advantages in handling data that are irregularly spaced. Irregularly spaced longitudinal survey data have arisen in studies of circadian rhythms (Sherwood et al., 2001), finance (Vecchiato, 1997), physiological data (Pincus et al., 1991), and numerous other studies involving ecological momentary assessments, experience sampling and daily diary designs (Bolger et al., 2003; Schwartz & Stone, 1998).

Third, the proposed RS-DE framework extends conventional DE modeling by allowing the inclusion of multiple regimes and DE functions within regimes. The inclusion of a DE model within each regime also renders RS-DE models different from another class of well-known longitudinal models of discrete changes—the hidden Markov models (Elliott et al., 1995), or the related latent transition models (which emphasize categorical indicators; Collins and Wugalter, 1992; Lanza & Collins, 2008). In particular, the specification of a continuous-time model of change within each regime allows the dynamics within regimes to unfold in a continuous fashion, even though the shifts between regimes or classes are discrete. Thus, the proposed modeling framework is suited for representing processes whose changes within regimes are smooth and evolve continuously over time—except at particular, unknown transition points. This feature is distinct from hidden Markov models, which target primarily systems that undergo discontinuous shifts between conceptually disparate phases that could have very different mean levels, covariance structures, item measurement characteristics, and so on.

The remainder of the article is organized as follows. We first describe in more detail the empirical example that motivated us to develop the RS-DE model and associated estimation technique described in the present article. We then present the broader modeling framework that can handle other modeling extensions similar to the model considered in our motivating example and briefly review an R package, *dynr* (Ou et al., 2016), that offers an R interface for implementing and fitting these models. We provide an overview of the associated estimation procedures, followed by a summary of the results from empirical model fitting, as well as a targeted Monte Carlo simulation study designed to test the feasibility of using well-known information criterion (IC) measures to compare the fit of models positing different numbers of regimes. We conclude with some remarks on the strengths and limitations of the proposed technique.

1. Motivating Example

One important developmental milestone in a secure infant's first year of life is to be able to alternate periods of close contacts with their mothers (e.g., being held, cuddling) and actions to explore the environment (e.g., learning to walk). This does not only underscore the importance

of studying the temporal structure of an infant's behaviors, but also the variability in a mother–infant dyad's interactive dynamics over time. In the motivating data set, observable behaviors of $n = 29$ dyads during the SSP (Ainsworth et al., 1978) from a larger study were recorded with four synchronized Microsoft Kinect sensors (Sivalingam et al., 2012) when the infants were 12 months of age. The Kinect is an economical, widely available sensor that incorporates both depth and high-definition video cameras. The depth camera captured continuous 3-dimensional (3D) information about the position and orientation of each infant's and mother's head movements, and high-definition video cameras were used to capture the infant's facial expression. Audio was recorded with a LENA (Language ENvironment Analysis) system that includes a two-ounce digital recorder that the infant wore in a specially constructed vest. After removing participants with excessive missingness (e.g., due to technical difficulties in capturing the head movements and in the recording of other covariates, as well as insufficient variability in the corresponding variables), a total of $n = 29$ dyads were used for modeling purposes.

The SSP consisted of eight 3-minute episodes including two separations from the mother, each followed by a reunion. Separations (but not reunions) were curtailed if an infant was extremely distressed (e.g., 60 seconds of crying Waters, 2002). Frame-by-frame data from the two reunion sessions were down-sampled, aggregated, and synchronized with the LENA audio recordings to yield a range of 112 to 1418 (mean = 1055.77, SD = 220) total number of time points within each dyad and reunion session, with adjacent time points separated by .003 minutes (0.18 second). Based on the Kinect measurements of the x-, y-, and z- Cartesian coordinates of the each dyad member's head position in the room in a 3-D space at time $t_{i,j}$, we computed the relative locations of the dyad members in the room as the Euclidean distance (specifically, norm) of each individual's distance (in meters) from a common point in the room—a chair for the mother to sit, at which $x = y = z = 0$, as $\sqrt{(x-0)^2 + (y-0)^2 + (z-0)^2}$, for each person and time point. The key idea behind how the x-, y- and z- coordinates of each dyad member indicated the location of that dyad member in a 3-D space (i.e., the experimental room), and how the equation for the Euclidean norm revealed the distance between the two dyad members, are shown in Fig. 1. As opposed to computing the Euclidean distances of the dyad members from each other and using that as the sole dependent variable in a univariate dynamic model, we used the dyad members' respective distances from the chair to yield two dependent variables (relative locations of the mother and the infant, respectively) for fitting a series of bivariate dynamic models. Doing so allows us to represent distinct dynamic behaviors manifested by each dyad member, including the disentanglement of mother-initiated Proximity-Seeking behavior from infant-initiated Proximity-Seeking behavior.

The resultant mother- and infant-specific Euclidean measures are shown in Fig. 2. Plots of the infants' as well as mothers' distances from the chair (at 0) in meters are shown in Fig. 2 over minutes. As seen in Fig. 2c, d, most mothers in the study, upon entering the room, progressed to the chair at different speeds after different degrees of interaction with the infants. Some infants alternated between being close to the mother sitting at the chair and spending time away from her, whereas other infants remained close to their mother throughout the reunion session. Distances of less than 1 meter between an infant and the mother reflect instances where the mother and the infant were physically close to each other.

In the present dataset, there was insufficient variability in infant attachment to warrant examination of individual differences in interactive dynamics due to differences in infant attachment style. Thus, we focus on evaluating the dynamics of infant and mother within the reunion sessions, as well as differences in dynamics between the first and second reunion sessions. In the SSP, the infants were exposed—not once but twice—to a potentially stressful and anxiety-provoking social situation, namely being separated from the mother. The cumulation of stress from the first to the second reunion session is purported to trigger Proximity-Seeking behavior, particularly among infants with high risk factors (e.g., those with insecure attachment). However, previous data from the SSP procedure have simply been used to code infants into those with secure vs. other insecure

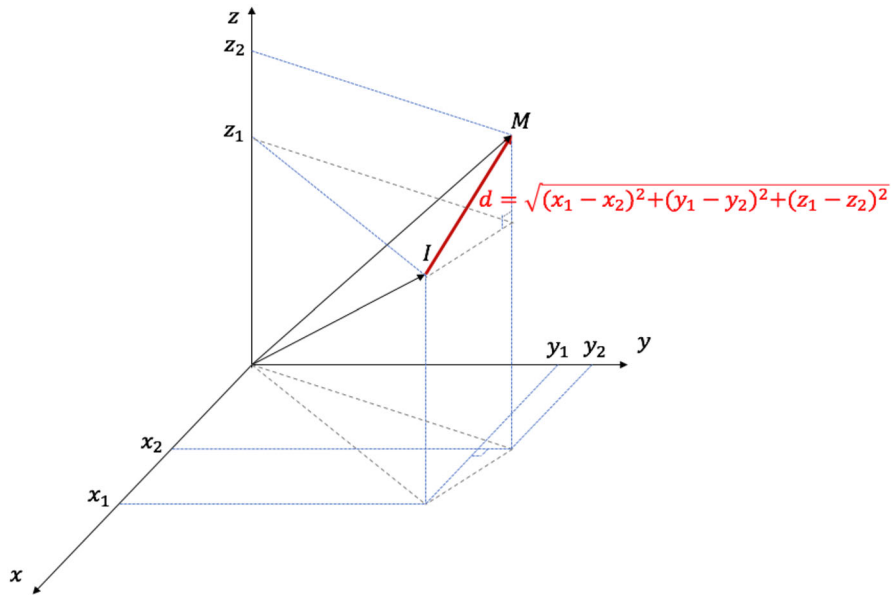$$d = \sqrt{(x_1 - x_2)^2 + (y_1 - y_2)^2 + (z_1 - z_2)^2}$$

FIGURE 1.

Let points I and M represent the respective locations of the infant and mom in a 3-dimensional space (e.g., the experimental room in the SSP) defined by the x-, y-, and z- Cartesian coordinates, each perpendicular to another. If the position of I is at (x_1, y_1, z_1) and that of M is at (x_2, y_2, z_2), then the distance d between I and M can be calculated as the Euclidean distance, $\sqrt{(x_1 - x_2)^2 + (y_1 - y_2)^2 + (z_1 - z_2)^2}$. To consolidate the x, y, and z coordinates into a single measure indicating the relative location of each dyad member in the room, we computed the Euclidean distance of each of I and M from the origin (the chair's position in the context of the motivating example, at which $x = y = z = 0$).

attachment styles. In other words, the rich information that defines the very essence of secure vs. insecure behavior—including intra- and inter-dyad dynamics manifested by the mothers and infants, and the corresponding between-session differences—is all reduced to a single, categorical rating of security for each infant.

Our first proposed model was motivated by our intention to "return to the roots" of modeling attachment dynamics. In particular, we were interested in examining differences in infant- and mother-initiated Proximity-Seeking behaviors both within and between the reunion sessions, and changes in the dyads' probabilities of transitioning between the Proximity-Seeking and Exploration regime from the first to the second reunion session. Based on Fig. 2a–d, it can be seen that from the first to the second reunion session, more infants (see panels (a) and (b)) as well as mothers (see panels (c) and (d)) tended to stay close to the chair in the second as compared to the first reunion session. In Fig. 3a–d, we show the time series plots of the Euclidean distances of two dyads with low (less than 5% of the reunion episodes) and high (more than 95% of the reunion episodes) proportions of infant vocalizations, respectively, as measured by the LENA. At 12 months, infant vocalizations during the SSP mostly index fussing and crying, with some occasional babbling. The plots indicate that the infant with a low overall proportion of infant vocalizations (i.e., low distress; depicted in panels (a) and (b)) was more likely to alternate between Exploration and Proximity-Seeking than the infant with a high overall proportion of infant vocalizations (i.e., high distress; see panels (c) and (d)), who essentially trailed behind the mother wherever she went. Furthermore, there is an increased tendency for the first dyad to engage in more Proximity-Seeking behavior in the second than in the first reunion session. The extent to which the Proximity-Seeking behavior was initiated predominantly by the mother or the infant was unclear, but could be clarified with results from our proposed model.
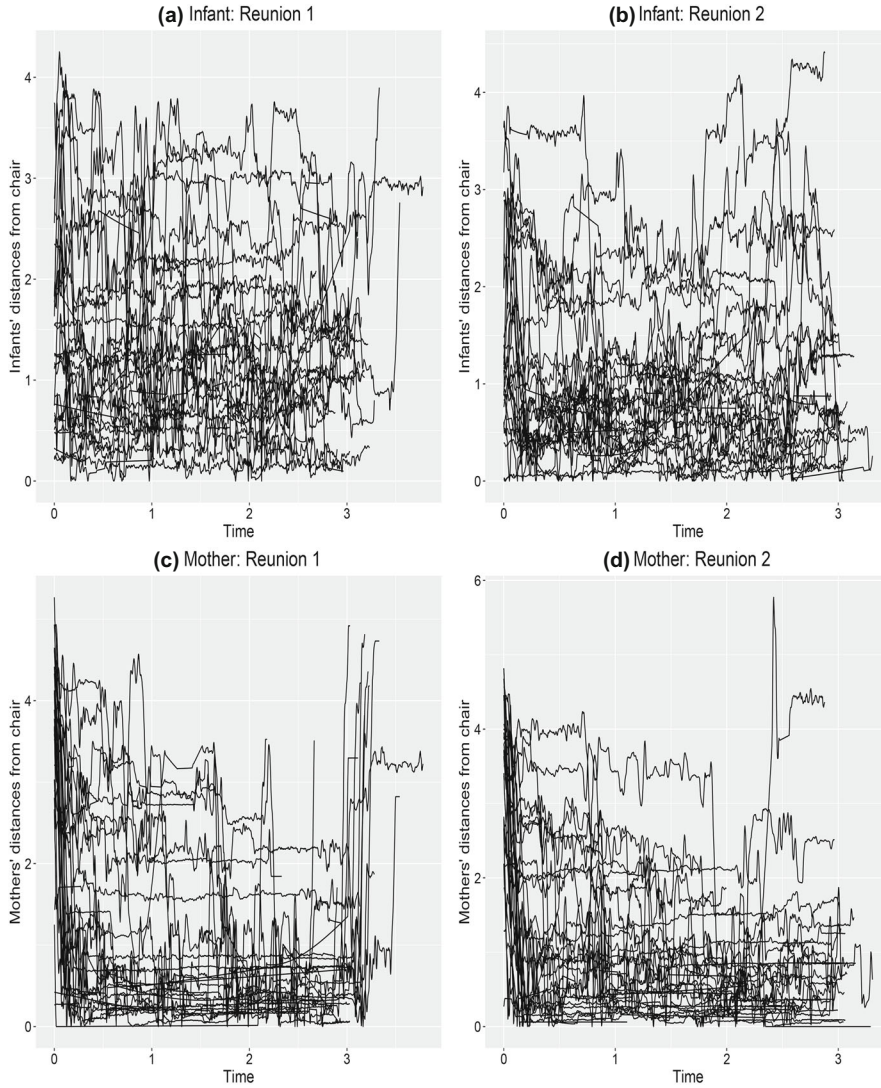
FIGURE 2.

a–d: Plots of the infants' and mothers' Euclidean distances (in meters) from a chair positioned in the room for the mothers to sit during the two reunion sessions of the SSP. The time scale depicted here represents time in minutes.

Our first proposed model posits that the ith mother–infant dyad during reunion session g would transition between two regimes as dictated by a person- and time-varying but unobserved regime indicator, $S_{ig}(t)$. Here, (t) may be any real- or integer-valued number indexing time at any arbitrary point; i indexes person and g indexes reunion session ($g = 1, 2$). The two regimes are denoted, respectively, as the *Exploration* regime ($S_{ig}(t) = 1$) and the *Proximity-Seeking* regime ($S_{ig}(t) = 2$), within which the dynamics, were postulated as:

$$\frac{\mathrm{d}Mom_{ig}(t)}{\mathrm{d}t} = -r_{1,S_{ig}(t)}Mom_{ig}(t) + a_{12,S_{ig}(t)}[Infant_{ig}(t) - Mom_{ig}(t)]$$

$$\frac{\mathrm{d}Infant_{ig}(t)}{\mathrm{d}t} = -r_{2,S_{ig}(t)}[Infant_{ig}(t) - setpoint_{ig}] + a_{21,S_{ig}(t)}[Mom_{ig}(t) - Infant_{ig}(t)]$$

(a) ID = 37: Reunion 1

(b) ID = 37: Reunion 2

(c) ID = 53: Reunion 1
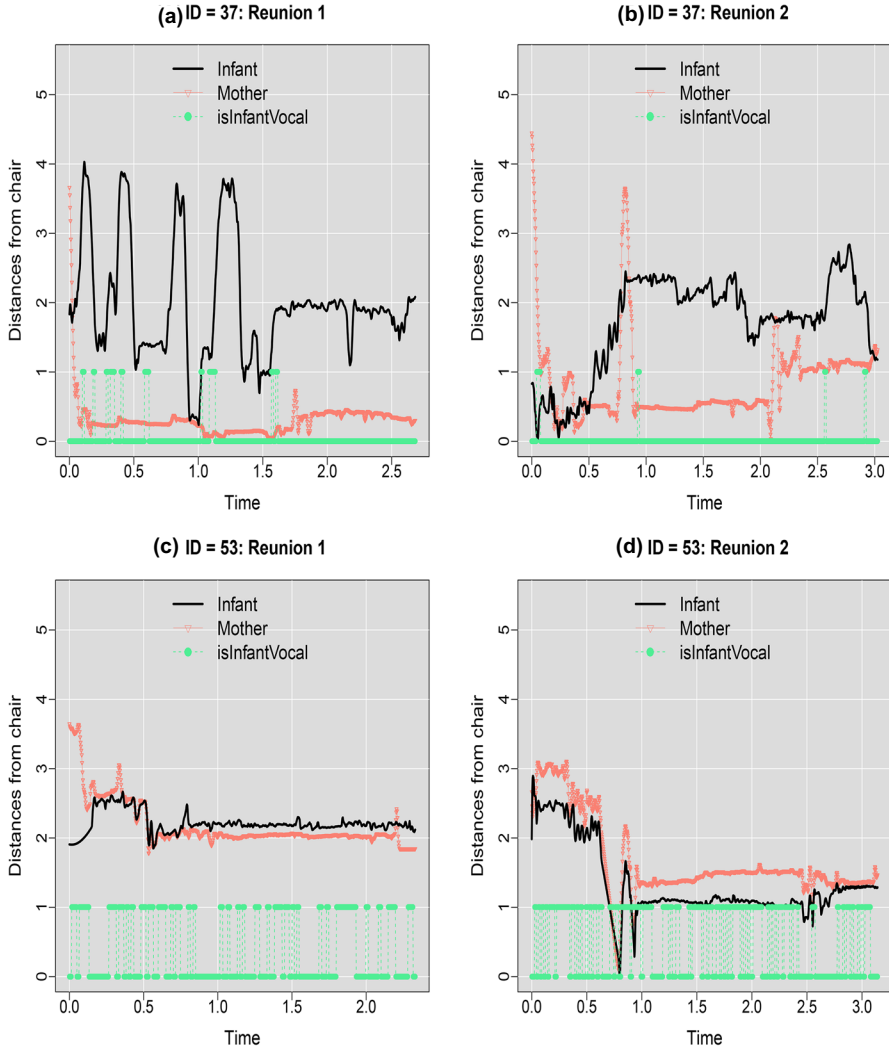
(d) ID = 53: Reunion 2

FIGURE 3.

a–d Illustrative time series plots of the relative locations of two mother–infant dyads with low and high proportions of infant vocalizations over time, respectively, during the two reunion sessions.

$$
\begin{aligned}
r_{1,S_{ig}(t)}, r_{2,S_{ig}(t)} &\begin{cases} \geq 0 \text{ if } S_{ig}(t) = 1 & \text{Exploration} \\ = 0 \text{ if } S_{ig}(t) = 2 & \text{Proximity-Seeking} \end{cases} \\
a_{12,S_{ig}(t)}, a_{21,S_{ig}(t)} &\begin{cases} = 0 \text{ if } S_{ig}(t) = 1 & \text{Exploration} \\ \geq 0 \text{ if } S_{ig}(t) = 2 & \text{Proximity-Seeking.} \end{cases}
\end{aligned} \tag{1}
$$

That is, we hypothesized that when the dyads were in the Exploration regime ($S_{ig}(t) = 1$), the parameters $r_{1,1}$ and $r_{2,1}$ represent the average rates at which the mothers and the infants approached their respective set-points. For the mother, the set-point corresponded to the location of the chair, which was located at the value of zero; for the infant, this was captured by the person-specific term, $setpoint_i$, corresponding to the location at which the infant lingered to play with toys in the room while being away from the mother. Thus, the parameters $r_{1,1}$ and $r_{2,1}$ may be regarded as the mothers' and infants' overall *divergence rates* from each other during the Exploration regime.

These divergence parameters were constrained to be nonnegative (≥ 0) in the Exploration regime on theoretical grounds.[1] Specifically, when $r_{1,1}$ is positive, a positive distance from zero for mother (i.e., $Mom_{ig}(t)$) leads to a negative rate of change, $\frac{dMom_{ig}(t)}{dt}$. Such negative rate of change, in turn, leads to a decline in the mother's Euclidean distance from the chair at the next time point. Similarly, when $r_{2,1}$ is positive and an infant's relative location is above his/her set-point (i.e., the infant is further away from the chair than his/her set-point), this entails a negative rate of change, $\frac{dInfant_{ig}(t)}{dt}$, and in turn, a subsequent decline in the infant's relative location to move closer to the set-point. A negative distance from the set-point, in contrast, indicates that the infant's relative location is lower than his/her set-point. This yields a positive rate of change in infant that leads to an increase in the infant's relative location to get closer to the set-point. Thus , when $r_{1,1}$ and $r_{2,1}$ are positive, they dictate the rates at which mothers and infants approach their respective set-points (the chair and the location of $setpoint$); or in other words, the rates at which they diverge from each other. Negative values of these parameters would lead to explosive dynamics (specifically, exponential divergence of each dyad member from his/her set-point), which we did not expect to see based on the nature of the empirical data and the task (participants were in a room—a constrained space). The changes in location would stop when the rates of change are zero, which occur when the child is at the set-point, $setpoint$, and the mother is at the chair (0).

The corresponding divergence rates while in the Proximity-Seeking regime, $r_{1,2}$ and $r_{2,2}$, were set to zero to define the nature of the Proximity-Seeking regime as a within-dyad phase during which the dyads were not "exploring" the room but rather were seeking the proximity of (or were "coupled to") the other dyad member. The parameters $a_{12,m}$ and $a_{21,m}$ reflect the extent to which the mothers and the infants were coupled to each other, respectively, during regime m. As such, they are denoted herein as the *Proximity-Seeking* or *coupling* strengths of the dyads during regime m. These parameters were set to zero in the Exploration regime ($m = 1$) and were specified to be nonnegative but freely estimated in the Proximity-Seeking regime ($m = 2$) on theoretical grounds. Specifically, when these parameters are positive, a positive distance from *the other* dyad member leads to a positive rate of change for a dyad member and subsequently, movements away from the chair to approach the other dyad member. This occurs, for example, when $Infant_{ig}(t) - Mom_{ig}(t) > 0$ in the equation for the mother in (1), corresponding to the scenario where the infant is further away from the chair, and the mother's subsequent movements from a position that is closer to the chair to approach the infant. Movements in the reverse direction would occur when there is a negative distance between a dyad member and the other dyad member, leading the two dyad members to get closer to each other again. The changes in location would stop when the rates of change are zero: occurring when the distance between the two dyad members is zero, namely when $Infant_{ig}(t) - Mom_{ig}(t) = Mom_{ig}(t) - Infant_{ig}(t) = 0$, and $r_{1,m} = r_{2,m} = 0$. Negative values of $a_{12,m}$ and $a_{21,m}$, in contrast, would dictate that the two members move further *away* from each other when there is any distance between them. This contradicts the fundamental definition of the Proximity-Seeking regime and would lead to estimation difficulties in distinguishing the Exploration regime from the Proximity-Seeking regime. In addition, by representing the mother–infant dyad as a bivariate system of equations, we were able to use the parameters $a_{12,2}$ and $a_{21,2}$ while the dyads were in the Proximity-Seeking regime to distinguish between the rates of mother-initiated (as reflected by $a_{12,2}$) and infant-initiated (as revealed by $a_{21,2}$) Proximity-Seeking behavior. Here, we conceptualized and represented the dynamics of the dyads from the two sessions as a two-group model. Selected dynamic parameters, such as $a_{12,2}$ and $a_{21,2}$, could be constrained to be invariant across reunion sessions as shown in Eq. (1), or allowed to vary between the two reunion sessions (i.e., between

---

[1]This was accomplished by optimizing the log transformations of these parameters on an unconstrained scale, and upon convergence, obtaining the standard error estimates of the final, transformed (constrained) parameters via the delta method (Casella & Berger, 2001).

"groups") to test targeted hypotheses concerning the within-dyad deviations in dynamics across sessions.

The true scores in dyad i's mother and infant head positions, denoted in the equations above as $Mom_{ig}(t)$ and $Infant_{ig}(t)$, respectively, are each indicated by the observed Euclidean measure derived from the Kinect measurements to yield a measurement equation at each observed time point $t_{i,j}$ in reunion session g, as

$$y_{Mom,ig}(t_{i,j}) = Mom_{ig}(t_{i,j}) + e_{Mom,ig}(t_{i,j}), \text{ and}$$
$$y_{Infant,ig}(t_{i,j}) = Infant_{ig}(t_{i,j}) + e_{Infant,ig}(t_{i,j}), \tag{2}$$

where $y_{Mom,ig}(t_{i,j})$ and $y_{Infant,ig}(t_{i,j})$ are empirically observed Euclidean measures of mother and child positions relative to the chair, respectively, and $e_{Mom,i}(t_{i,j})$ and $e_{Infant,i}(t_{i,j})$ are their respective independent and uncorrelated measurement errors with variances $\sigma^2_{e,Mom}$ and $= \sigma^2_{e,Infant}$.

A 2×2 transition probability matrix is then used to specify the probability that an individual is in a certain regime conditional on the previous regime. We estimate the transition probability functions using person- and session-specific covariates as:

$$
\begin{aligned}
\pi_{11} &= \Pr\left[\text{Exploration}_i(t_{i,j})|\text{Exploration}_i(t_{i,j-1}), \text{meanInfantVocal}_i, \text{isReunion2}_{ig}\right] \\
&= \frac{\exp(c_1 + c_{\Delta,11} + d_{11,1}\text{meanInfantVocal}_i + d_{11,2}\text{isReunion2}_{ig})}{\sum_{k=1}^{2} \exp(c_k + c_{\Delta,1k} + d_{1k,1}\text{meanInfantVocal}_i + d_{1k,2}\text{isReunion2}_{ig})} \\
&= \frac{\exp(c_1 + c_{\Delta,11} + d_{11,1}\text{meanInfantVocal}_i + d_{11,2}\text{isReunion2}_{ig})}{1 + \exp(c_1 + c_{\Delta,11} + d_{11,1}\text{meanInfantVocal}_i + d_{11,2}\text{isReunion2}_{ig})} \\
\pi_{21} &= \Pr\left[\text{Exploration}_i(t_{i,j})|\text{Proximity-Seeking}_i(t_{i,j-1}), \text{meanInfantVocal}_i, \text{isMomVocal}_i(t_{i,j})\right] \\
&= \frac{\exp(c_1 + d_{21,1}\text{meanInfantVocal}_i + d_{21,2}\text{isReunion2}_{ig})}{1 + \exp(c_1 + d_{21,1}\text{meanInfantVocal}_i + d_{21,2}\text{isReunion2}_{ig})}.
\end{aligned}
\tag{3}
$$

where meanInfantVocal_i is the average proportion of infant vocalization in dyad i across both reunion sessions, whereas isReunion2_{ig} is a binary indicator of whether session g for dyad i is the first ($= 0$) or second ($= 1$) reunion session. The two equations above depict, from time $t_{i,j-1}$ to $t_{i,j}$, the probability of staying within the Exploration regime, as well as the probability of switching from the Proximity-Seeking regime to the Exploration regime. Designating the second regime (the Proximity-Seeking regime) as the reference regime, the parameter c_1 is an intercept parameter that governs the log odds (LO) for the dyads to switch into the Exploration regime from the Proximity-Seeking (reference) regime during the first reunion session when $meanInfantVocal_i = 0$. The deviation parameter, $c_{\Delta,11}$, which appears in the π_{11} function, represents the first reunion session's deviation in LO of switching into the Exploration regime from the Exploration regime relative to c_1 (i.e., the LO of switching into it from the reference regime) when $meanInfantVocal_i = 0$. The corresponding deviation in LO for the second reunion session is given by $c_{\Delta,11} + d_{11,2}$. Finally, the coefficients $d_{11,1}$ and $d_{21,1}$ show the effects of $meanInfantVocal$ on the LO of staying within the Exploration regime (and thus, π_{11}), and the LO of switching from the Proximity-Seeking regime to the Exploration regime (and correspondingly, π_{21}), controlling for $meanInfantVocal_i$.

The simplifications of the denominators of these transition probability equations from the first to the second step arise because of the constraints $c_2 = c_{\Delta,12} = d_{12,1} = d_{12,2} = d_{22,1} = d_{22,2} = 0$, needed to ensure that the remaining parameters can be uniquely identified. Imposing these constraints is one of the many possible parameterizations to ensure that the sum of each row of the transition probability matrix, including $\pi_{11} + \pi_{12}$ as well as $\pi_{21} + \pi_{22}$, is equal to 1. Here, π_{12}

is the probability of transitioning from regime 1 to regime 2, and π_{22} is the probability of staying within regime 2. Because $\pi_{11} + \pi_{12} = \pi_{21} + \pi_{22} = 1$, we can also obtain π_{12} and π_{22} as 1-π_{11} and $1 - \pi_{21}$, respectively.

We also considered several adaptations and extensions of the model shown in (1) as motivated by several theoretical and data-driven reasons. For instance, we also compared the model in (1) to an alternative one-regime model, modeling variations to test targeted changes in dynamics between reunion sessions, and several other practical but admittedly, ad hoc adaptations of the model due to properties of the data. These adaptations are described in the simulation study and empirical illustration where appropriate.

2. RS-DE Modeling Framework

In this section, we discuss the broader regime-switching DE (RS-DE) modeling framework, of which the model shown in the motivating example can be viewed as a special case. Formally, we assume that the dynamic model within a particular regime takes on the form of an SDE model as

$$d\boldsymbol{\eta}_i(t) = \boldsymbol{f}_{S_i(t)}\left(\boldsymbol{\eta}_i(t), t, \boldsymbol{x}_i(t)\right) dt + d\boldsymbol{w}_i(t), \tag{4}$$

where i indexes the smallest independent unit of analysis (e.g., person, or dyad in the empirical example), t indexes time, and the notation "(t)" is a continuous index of time that may take on any real or integer value. $S_i(t)$ is a latent regime indicator of the operating regime at any arbitrary time t. $\boldsymbol{f}_{S_i(t)}(.)$ is a vector of regime-dependent, differentiable linear or possibly nonlinear drift functions that may depend on t, $\boldsymbol{\eta}_i(t)$, a $w \times 1$ vector of latent variables of interest at time t, and $\boldsymbol{x}_i(t)$, a vector of person- and time-varying covariates at time t. $\frac{d\boldsymbol{\eta}_i(t)}{dt}$ denotes the corresponding $w \times 1$ vector of first derivatives of $\boldsymbol{\eta}_i(t)$, and the latter may include latent derivative variables needed to define higher-order SDEs, namely SDEs involving higher-order derivatives than first derivatives. $\boldsymbol{w}(t)$ is a vector of Wiener processes (process noises or continuous-time counterpart of Brownian processes) with regime-specific diffusion matrix $\mathbf{Q}_{S_i(t)}$ and $d\boldsymbol{w}_i(t)$ denotes differences in the Wiener processes over dt.[2] The proposed model for the motivating example is a regime-switching linear ODE wherein $\mathbf{Q}_{S_i(t)}$ is equal to a null matrix for each of the hypothesized regimes.

The latent variables in $\boldsymbol{\eta}_i(t_{i,j})$ at discrete time point $t_{i,j}$ are indicated by a $p \times 1$ vector of manifest observations, $\boldsymbol{y}_i(t_{i,j})$, assumed to be measured at individual- (or dyad-) specific and possibly irregularly spaced time points $t = t_{i,j}$, $j = 1, \ldots, T_i$, as are the vector of person- and time-varying covariates, $\boldsymbol{x}_i(t_{i,j})$, and the latent regime indicator, $S_i(t_{i,j})$. The initial conditions for the SDEs are defined explicitly to be the latent variables at an initial time point, t_1 (e.g., the first observed time point), denoted as $\boldsymbol{\eta}_i(t_{i,1})$, and are specified to be normally distributed with means $\boldsymbol{\mu}_{\boldsymbol{\eta}_1}$ and covariance matrix, $\boldsymbol{\Sigma}_{\boldsymbol{\eta}_1}$. The time interval between time $t_{i,j}$ and $t_{i,j+1}$ is denoted as $\Delta_{i,j} = t_{i,j+1} - t_{i,j}$.

The vector of manifest observations is linked to the latent variables as

$$\boldsymbol{y}_i(t_{i,j}) = \boldsymbol{\tau}_{S_i(t_{i,j})} + \boldsymbol{\Lambda}_{S_i(t_{i,j})}\boldsymbol{\eta}_i(t_{i,j}) + \mathbf{A}_{S_i(t_{i,j})}\boldsymbol{x}_i(t_{i,j}) + \boldsymbol{\epsilon}_i(t_{i,j}),$$
$$\boldsymbol{\epsilon}_i(t_{i,j}) \sim N\left(\mathbf{0}, \mathbf{R}_{S_i(t_{i,j})}\right), \tag{5}$$

where $\boldsymbol{\tau}_{S_i(t_{i,j})}$ is $p \times 1$ vector of intercepts, $\mathbf{A}_{S_i(t_{i,j})}$ is a matrix of regression weights for the covariates in $\boldsymbol{x}_i(t_{i,j})$ observed at time $t_{i,j}$, and $\Lambda_{S_i(t_{i,j})}$ is a $p \times w$ factor loading matrix that links

---

[2]An alternative form of Eq. 4 that may be easier to understand is one where all components of the equation are divided by dt, yielding the first derivatives of elements in $\boldsymbol{\eta}_i(t)$, namely, $\frac{d\boldsymbol{\eta}_i(t)}{dt}$, on the left-hand side of Eq. (4). The expression shown in 4 is, in the so-called Ito form, often adopted to highlight explicitly that the Wiener process is not differentiable with respect to time (i.e., $\frac{d\boldsymbol{w}_i(t)}{dt}$ is not defined as dt approaches zero; Arnold, 1974, Molenaar & Newell, 2003).

the observed variables to the latent variables. Adopting the modeling tradition in the state-space literature (see, e.g., Durbin & Koopman, 2001), we assume that all sources of time dependencies of interest are specified as part of the dynamic model in (4) and consequently, $\boldsymbol{\epsilon}_i(t_{i,j})$ is a $p \times 1$ vector of measurement errors assumed to be serially uncorrelated over time and normally distributed with a mean vector of zeros and regime-dependent covariance matrix, $\mathbf{R}_{S_i(t_{i,j})}$.

Equations 4 and 5 are the *dynamic model* and *measurement model* that defines a dynamic system, respectively. The former describes the ways in which the latent variables change over time, whereas the latter portrays the relationships between a set of observed variables and a set of latent variables over time. The subscript $S_i(t_{i,j})$ associated with $\boldsymbol{\tau}_{S_i(t_{i,j})}$, $\boldsymbol{\Lambda}_{S_i(t_{i,j})}$, $\mathbf{A}_{S_i(t_{i,j})}$, and $\mathbf{R}_{S_i(t_{i,j})}$ indicates that the values of some of the parameters in them may depend on $S_i(t_{i,j})$, the operating regime for individual (dyad) i at a particular observed time $t_{i,j}$. In practice, not all of these elements are free to vary by regime. Our motivating example illustrated one example of such constrained models. Other than allowing some parameters to differ in values as conditional on changes in $S_i(t_{i,j})$, the model is used to describe the dynamics of multiple subjects (dyads) at the group level. Thus, when there is only one regime, these parameters do not differ in values over individuals (dyads) or time, unless the hypothesized variations in parameters are explicitly integrated into the dynamic model, for example, as random effects characterizing between-individual (or between-dyad) differences.

When there is no regime dependency, Eqs. 4 and 5 can be conceived as a linear/nonlinear SDE model with Gaussian distributed measurement errors. To make inferences on $S_i(t_{i,j})$, it is essential to specify a model or mechanism through which $S_i(t_{i,j})$ changes over individuals and time. Here, the initial regime probabilities for $S_i(t_{i,1})$ are represented using a multinomial regression model as

$$\Pr\left(S_i(t_{i,1}) = m | \boldsymbol{x}_i(t_{i,1})\right) \overset{\Delta}{=} \pi_{m,i1} = \frac{\exp(a_m + \mathbf{b}_m^T \boldsymbol{x}_i(t_{i,1}))}{\sum_{k=1}^{M} \exp(a_k + \mathbf{b}_k^T \boldsymbol{x}_i(t_{i,1}))}, \tag{6}$$

where M denotes the total number of regimes, a_m denotes the logit intercept for the mth regime and $\mathbf{b}_m$ is a vector of regression slopes linked to $\boldsymbol{x}_i(t_{i,1})$, the vector of covariates that also appears in Eqs. (4–5), but is now restricted to include covariates at $t_{i,1}$ only to explain possible interindividual or between-dyad differences in initial conditions. For identification purposes, we set a_M and all elements in $\mathbf{b}_M$ to 0 for the reference (last) regime to ensure that the initial regime probabilities across the M regimes sum to 1.0.

In a similar vein, a first-order Markov process conforming to a multinomial logistic regression equation is assumed to govern the probabilities of transitioning between regimes:

$$\Pr\left(S_i(t_{i,j}) = m | S_i(t_{i,j-1}) = l, \boldsymbol{x}_i(t_{i,j})\right) \overset{\Delta}{=} \pi_{lm,it} = \frac{\exp(c_m + c_{\Delta,lm} + \mathbf{d}_{lm}^T \boldsymbol{x}_i(t_{i,j}))}{\sum_{k=1}^{M} \exp(c_k + c_{\Delta,lk} + \mathbf{d}_{lk}^T \boldsymbol{x}_i(t_{i,j}))}, \tag{7}$$

where $\pi_{lm,it}$ denotes individual (dyad) i's probability of transitioning from regime l at time $t_{i,j-1}$ to regime m at time $t_{i,j}$, c_m denotes the logit intercept for the mth regime, $c_{\Delta,lm}$ denotes the deviation in LO of switching into latent regime m at time $t_{i,j}$ from latent regime l (i.e., from $S_i(t_{i,j-1}) = l$ to $S_i(t_{i,j}) = m$), as compared to switching into latent regime m from the reference regime, i.e., $S_i(t_{i,j-1}) = M$; $\mathbf{d}_{lm}$ is a vector of logit slopes summarizing the effects of the covariates in $\boldsymbol{x}_i(t_{i,j})$ on the deviations in LO of switching into regime m from regime l as opposed to from the reference regime M. For identification purposes, we impose the constraints that $c_M = c_{\Delta,lM} = 0$ and $\mathbf{d}_{lM} = \mathbf{0}$ for $l = 1, \ldots, M$ to ensure that $\sum_{m=1}^{M} \pi_{lm} = 1$.

To summarize, the parameters in Eqs. 6–7, including $a_m, c_m, c_{\Delta,lm}$, and those in $\mathbf{b}_m$ and $\mathbf{d}_{lm}$ for $l = 1, \ldots, M$ and $m = 1, \ldots, M$ are regarded as model parameters that are to be estimated

with other parameters that appear in $\boldsymbol{\tau}_{S_i(t_{i,j})}$, $\Lambda_{S_i(t_{i,j})}$, $\mathbf{b}_{S_i(t_{i,j})}$, $\mathbf{A}_{S_i(t_{i,j})}$, and $\mathbf{R}_{S_i(t_{i,j})}$ in Eqs. 4 and 5. The procedures for estimating these parameters, collected into the vector $\boldsymbol{\theta}$, are outlined next.

3. Estimation Procedures

We use the *continuous-discrete time extended Kim filter* (CDEKimF) algorithm, provided as part of the R package, *Dyn*amic Modeling in *R* (*dynr*; Ou et al., 2016), to estimate the unknown components of the model summarized in Eqs. (4)—(5). The CDEKimF essentially combines the continuous–discrete extended Kalman filter (CDEKF; Bar-Shalom et al., 2001; Kulikov & Kulikova, 2014; Kulikova & Kulikov 2014), which can be used to estimate the latent variables that appear in Eqs. (4) – (5) when there is only a single regime, and the Kim filter (Kim & Nelson, 1999), which includes procedures for handling the estimation of $S_i(t_{i,j})$.

Before we elaborate further on features of the CDEKimF, some clarifications of notation and links to relevant work in the literature are in order. Let $\mathbf{Y}_i(t_{i,j})$ denote all the manifest observations from $t_{i,1}$, ..., up to $t_{i,j}$; $\hat{\boldsymbol{\eta}}_i(t_{i,j}|t_{i,j-1}) = E(\boldsymbol{\eta}_i(t_{i,j})|\mathbf{Y}_i(t_{i,j-1}))$ and $\mathbf{P}_i(t_{i,j}|t_{i,j-1}) = Cov[\boldsymbol{\eta}_i(t_{i,j})|\mathbf{Y}_i(t_{i,j-1})]$ denote the predicted mean and covariance matrix of the latent variables, respectively, at time $t_{i,j}$ conditional on $\mathbf{Y}_i(t_{i,j-1})$, all the prior observations up to time $t_{i,j-1}$. In addition, we define $\hat{\boldsymbol{\eta}}_i(t_{i,j}|t_{i,j}) = E(\boldsymbol{\eta}_i(t_{i,j})|\mathbf{Y}_i(t_{i,j}))$ and $\mathbf{P}_i(t_{i,j}|t_{i,j}) = Cov[\boldsymbol{\eta}_i(t_{i,j})|\mathbf{Y}_i(t_{i,j})]$ as the filtered or updated mean and covariance matrix of the latent variables, respectively, at time $t_{i,j}$ conditional on $\mathbf{Y}_i(t_{i,j})$, all the observations up to time $t_{i,j}$. Finally, if data from all measurement occasions are available for estimation purposes, then all observations from each person (dyad) across all time points, $\mathbf{Y}_i(T_i)$, can be used to perform smoothing on the latent variable estimates to yield estimates of the means and covariance matrix of $\boldsymbol{\eta}_i(t_{i,j})$ conditional on all observations in $\mathbf{Y}_i(T_i)$, namely, $E(\boldsymbol{\eta}_i(t_{i,j})|\mathbf{Y}_i(T_i))$ and $\mathbf{P}_i(t_{i,j}|T_i) = Cov[\boldsymbol{\eta}_i(t_{i,j})|\mathbf{Y}_i(T_i)]$. Estimates of $\boldsymbol{\eta}_i(t_{i,j})$ obtained for time $t_{i,j}$ using observations from up to time $t_{i,j-1}$, up to time $t_{i,j}$, and up to time T_i are referred to, respectively, as the predicted, filtered (or updated), and smoothed latent variable estimates.

Overall, the implementation of the CDEKimF can be summarized into 4 basic steps (see Table 1), which we describe briefly below. Further technical details are summarized in the Supplementary Material section.

Step 1. CDEKF with prediction and update stages by regime. Even though the procedures that constitute the novel CDEKimF algorithm may be unfamiliar to most psychometricians, Step 1 of the CDEKimF algorithm can essentially be regarded as a latent variable (factor) score estimator whose linear and discrete-time analog has some known parallels to well-known factor score estimators in the psychometric literature (Chow et al., 2010; Dolan & Molenaar, 1991; Lawley & Maxwell, 1971; Oud et al., 1990). In the presence of multiple regimes, the purported latent variable estimation procedures—consisting of a series of prediction and update steps for all time points and individuals—now have to be performed as conditional on the current and previous operating regimes of a system. Thus, execution of the prediction and update procedures in Step 1 generally yields the output summarized in Table 1 under "Step 1" as conditional on $S_i(t_{i,j}) = m$ and $S_i(t_{i,j-1}) = l$. For now, we assume that Step 1 is run conditional on a set of fixed and known parameter values, $\hat{\boldsymbol{\theta}}$. After describing Steps 1–3, we will briefly summarize how these steps collectively yield by-products that may be used to construct a log-likelihood function that can be optimized for estimating $\boldsymbol{\theta}$.

In the continuous–discrete time context, the prediction step in the CDEKimF serves to compute $\hat{\boldsymbol{\eta}}_i(t_{i,j}|t_{i,j-1})$ and $\mathbf{P}_i(t_{i,j}|t_{i,j-1})$ by solving the ODEs (Kalman & Bucy, 1961; Jazwinski, 1970; Bar-Shalom et al., 2001; Kulikov & Kulikova, 2014; Kulikova & Kulikov 2014):

$$\frac{d\hat{\boldsymbol{\eta}}_i(t)}{dt} = \boldsymbol{f}_{S_i(t)}\left(\hat{\boldsymbol{\eta}}_i(t), t, \boldsymbol{x}_i(t)\right), \text{ and} \tag{8}$$

TABLE 1.
A summary of the products from running the four steps of proposed CDEKimF procedures with smoothing.

Products	Meanings
$\mathbf{Y}_i(t_{i,j})$	$\{\boldsymbol{y}_{i1}, \boldsymbol{y}_{i2}, \ldots, \boldsymbol{y}_i(t_{i,j})\}$
Steps 1–3 are performed for all of $t_{i,j}$, $i = 1, \ldots, n$; $j = 1, \ldots, T_i$	
Step 1: The CDEKF with prediction and update stages by regime for	
$\hat{\boldsymbol{\eta}}_i(t_{i,j}|t_{i,j-1})^{l,m}$	$E[\boldsymbol{\eta}_i(t_{i,j})|S_i(t_{i,j-1}) = l, S_i(t_{i,j}) = m, \mathbf{Y}_i(t_{i,j-1})]$
$\hat{\boldsymbol{\eta}}_i(t_{i,j}|t_{i,j})^{l,m}$	$E[\boldsymbol{\eta}_i(t_{i,j})|S_i(t_{i,j-1}) = l, S_i(t_{i,j}) = m, \mathbf{Y}_i(t_{i,j})]$
$\mathbf{P}_i(t_{i,j}|t_{i,j-1})^{l,m}$	$\mathrm{Cov}[\boldsymbol{\eta}_i(t_{i,j})|S_i(t_{i,j-1}) = l, S_i(t_{i,j}) = m, \mathbf{Y}_i(t_{i,j-1})]$
$\mathbf{P}_i(t_{i,j}|t_{i,j})^{l,m}$	$\mathrm{Cov}[\boldsymbol{\eta}_i(t_{i,j})|S_i(t_{i,j-1}) = l, S_i(t_{i,j}) = m, \mathbf{Y}_i(t_{i,j})]$
$v_i(t_{i,j})^{l,m}$	$\mathbf{Y}_i(t_{i,j}) - E[\mathbf{Y}_i(t_{i,j})|S_i(t_{i,j-1}) = l, S_i(t_{i,j}) = m, \mathbf{Y}_i(t_{i,j-1}), \mathbf{x}(t_{i,j})]$
$V_i(t_{i,j})^{l,m}$	$\mathrm{Cov}(\mathbf{Y}_i(t_{i,j}) - E[\mathbf{Y}_i(t_{i,j})|S_i(t_{i,j-1}) = l, S_i(t_{i,j}) = m, \mathbf{Y}_i(t_{i,j-1})])$
Step 2: The Hamilton filter	
$\mathrm{Pr}(S_i(t_{i,j})|\mathbf{Y}_i(t_{i,j}))$	Filtered regime probability for person (dyad) i at time $t_{i,j}$
Step 3: The collapsing procedure	
$\hat{\boldsymbol{\eta}}_i(t_{i,j}|t_{i,j})^m$	$E[\boldsymbol{\eta}_i(t_{i,j})|S_i(t_{i,j}) = m, \mathbf{Y}_i(t_{i,j})]$
$\mathbf{P}_i(t_{i,j}|t_{i,j})^m$	$\mathrm{Cov}[\boldsymbol{\eta}_i(t_{i,j})|S_i(t_{i,j}) = m, \mathbf{Y}_i(t_{i,j})]$
$v_i(t_{i,j})^m$	$\boldsymbol{y}_i(t_{i,j}) - E[\boldsymbol{y}_i(t_{i,j})|S_i(t_{i,j}) = m, \mathbf{Y}_i(t_{i,j-1}), \mathbf{x}(t_{i,j})]$
$V_i(t_{i,j})^m$	$\mathrm{Cov}(\boldsymbol{y}_i(t_{i,j}) - E[\mathbf{Y}_i(t_{i,j})|S_i(t_{i,j}) = m, \mathbf{Y}_i(t_{i,j-1})])$
Optional but needed for parameter estimation	
$\hat{\boldsymbol{\eta}}_i(t_{i,j}|t_{i,j})$	$E[\boldsymbol{\eta}_i(t_{i,j})|\mathbf{Y}_i(t_{i,j})]$
$\mathbf{P}_i(t_{i,j}|t_{i,j})$	$\mathrm{Cov}[\boldsymbol{\eta}_i(t_{i,j})|\mathbf{Y}_i(t_{i,j})]$
$\hat{\boldsymbol{\eta}}_i(t_{i,j}|t_{i,j-1})$	$E[\boldsymbol{\eta}_i(t_{i,j})|\mathbf{Y}_i(t_{i,j-1})]$
$\mathbf{P}_i(t_{i,j}|t_{i,j-1})$	$\mathrm{Cov}[\boldsymbol{\eta}_i(t_{i,j})|\mathbf{Y}_i(t_{i,j-1})]$
$v_i(t_{i,j})$	$\boldsymbol{y}_i(t_{i,j}) - E[\boldsymbol{y}_i(t_{i,j})|\mathbf{Y}_i(t_{i,j-1}), \mathbf{x}(t_{i,j})]$
$V_i(t_{i,j})$	$\mathrm{Cov}(\boldsymbol{y}_i(t_{i,j}) - E[\boldsymbol{y}_i(t_{i,j})|\mathbf{Y}_i(t_{i,j-1}), \mathbf{x}(t_{i,j})])$
Step 4: The smoothing procedure	
$\mathrm{Pr}(S_i(t_{i,j})|\mathbf{Y}_i(T_i))$	Smoothed regime probability for person (dyad) i at time $t_{i,j}$
$\hat{\boldsymbol{\eta}}_i(t_{i,j}|T_i)$	$E[\boldsymbol{\eta}_i(t_{i,j})|\mathbf{Y}_i(T_i)]$
$\mathbf{P}_i(t_{i,j}|T_i)$	$\mathrm{Cov}[\boldsymbol{\eta}_i(t_{i,j})|\mathbf{Y}_i(T_i)]$

$$\frac{\mathrm{d}\mathbf{P}_i(t)}{\mathrm{d}t} = \frac{\partial \boldsymbol{f}_{S_i(t)}\left(\hat{\boldsymbol{\eta}}_i(t), t, \boldsymbol{x}_i(t)\right)}{\partial \hat{\boldsymbol{\eta}}_i(t)}\mathbf{P}(t) + \mathbf{P}(t)\left(\frac{\partial \boldsymbol{f}_{S_i(t)}\left(\hat{\boldsymbol{\eta}}_i(t), t, \boldsymbol{x}_i(t)\right)}{\partial \hat{\boldsymbol{\eta}}_i(t)}\right)^{\top} + \mathbf{Q}_{S_i(t)} \quad (9)$$

with initial conditions $\hat{\boldsymbol{\eta}}_i(t_{i,j-1}) = \hat{\boldsymbol{\eta}}_i(t_{i,j-1}|t_{i,j-1})$ and $\mathbf{P}_i(t_{i,j-1}) = \mathbf{P}_i(t_{i,j-1}|t_{i,j-1})$, the updated latent variable estimates and the associated covariance matrix at time $t_{i,j-1}$. The Jacobian matrix $\frac{\partial \boldsymbol{f}_m(\hat{\boldsymbol{\eta}}_i(t), t, \boldsymbol{x}_i(t))}{\partial \hat{\boldsymbol{\eta}}_i(t)}$, consists of differentiation of the dynamic functions from the mth regime with respect to the latent variables in $\hat{\boldsymbol{\eta}}_i(t)$, evaluated at $\hat{\boldsymbol{\eta}}_i(t) = \hat{\boldsymbol{\eta}}_i(t_{i,j-1}|t_{i,j-1})$ and with the time-varying covariates in $\boldsymbol{x}_i(t)$ fixed at their observed values, $\mathbf{x}(t_{i,j})$. We use the fourth-order Runge–Kutta (Press et al., 2002) method to derive numerical solutions to Eqs. 8 and 9. Other numerical solvers, such as the adaptive ODE solvers, may also be used (Kulikov & Kulikova, 2014; Kulikova & Kulikov 2014).

During the *update* step, the prediction errors, $v_i(t_{i,j}) = \boldsymbol{y}_i(t_{i,j}) - \left[\boldsymbol{\tau}_{S_i(t_{i,j})} + \boldsymbol{\Lambda}_{S_i(t_{i,j})}\boldsymbol{\eta}_i(t_{i,j}) + \mathbf{A}_{S_i(t_{i,j})}\boldsymbol{x}_i(t_{i,j})\right]$ and its associate prediction error covariance matrix, $\mathbf{V}_i(t_{i,j}) = \Lambda_{S_i(t_{i,j})}\mathbf{P}_i(t_{i,j}|t_{i,j-1})\Lambda_{S_i(t_{i,j})}^{\top} + \mathbf{R}_{S_i(t_{i,j})}$, are computed and used to update the latent variable estimates to yield $\hat{\boldsymbol{\eta}}_i(t_{i,j}|t_{i,j})$ and $\mathbf{P}_i(t_{i,j}|t_{i,j})$.

Step 2. The Hamilton filter. Following Step 1, a procedure known as the Hamilton filter is executed in Step 2 to yield estimates of each individual's probabilities of being in each of the hypothesized regimes conditional on the data, namely $\Pr[S_i(t_{i,j}) = m|\mathbf{Y}_i(t_{i,j})]$ for all $t_{i,j}$. This procedure is summarized in Equations (S.5)–(S.9) in the Supplementary Material section. Such regime probability estimates convey information concerning the general unfolding of the different phases/regimes, including each individual's likelihood of staying within or transitioning between particular regimes, and the relative prevalence of the hypothesized regimes across time and individuals.

Step 3. The collapsing procedure. Step 1 of the CDEKimF generates M^2 new values of $\hat{\boldsymbol{\eta}}_i(t_{i,j}|t_{i,j})^{l,m}$ and $\mathbf{P}_i(t_{i,j}|t_{i,j})^{l,m}$ and their associated by-products at each time point for each individual. Storing all of these conditional estimates (e.g., for the purpose of computing log-likelihood values) can be computationally prohibitive in the presence of intensive longitudinal data. One way to circumvent this difficulty, as proposed by Kim & Nelson (1999), is to introduce a collapsing procedure to average over regime information from time $t_{i,j-1}$, yielding the estimates, $\hat{\boldsymbol{\eta}}_i(t_{i,j}|t_{i,j})^m$ (i.e., $E[\boldsymbol{\eta}_i(t_{i,j})|S_i(t_{i,j}) = m, \mathbf{Y}_i(t_{i,j})]$), and the associated covariance matrix, $\mathbf{P}_i(t_{i,j}|t_{i,j})^m$, by taking weighted averages of the $M \times M$ sets of latent variable estimates $\hat{\boldsymbol{\eta}}_i(t_{i,j}|t_{i,j})^{l,m}$ and their associated covariance matrices, $\mathbf{P}_i(t_{i,j}|t_{i,j})^{l,m}$ (with $l = 1, \ldots, M$, $m = 1, \ldots M$). Thus, Step 3 is generally a convenience step to reduce the computational burden of the algorithm and does not typically yield output that is of direct interest from an inferential standpoint.

Optional: Parameter estimation. Under the constraint of a linear measurement model, Chow and colleagues (2007; 2013) noted that the log-likelihood function, $\log[f(\mathbf{Y}; \boldsymbol{\theta})]$, can be computed using the prediction errors as

$$
\begin{aligned}
&\log[f(\mathbf{Y}; \boldsymbol{\theta})] \\
&= -\frac{1}{2} \sum_{i=1}^{n} \sum_{j=1}^{T_i} \left[p \log(2\pi) + \log|\mathbf{V}_i(t_{i,j})| + \boldsymbol{v}_i(t_{i,j})^\top \mathbf{V}_i(t_{i,j})^{-1} \boldsymbol{v}_i(t_{i,j}) \right],
\end{aligned}
\tag{10}
$$

where $\log[f(\mathbf{Y}; \boldsymbol{\theta})]$ is often referred to as the *prediction error decomposition* function (Schweppe, 1965) and it can be maximized using an optimization procedure of choice (e.g., Newton Raphson) to obtain estimates of $\boldsymbol{\theta}$. Standard errors associated with $\boldsymbol{\theta}$ can be obtained by taking the square root of the diagonal elements of $\mathbf{I}^{-1}$ at the convergence point, where $\mathbf{I}$ is the observed information matrix, obtained by computing the negative numerical Hessian matrix of $\log[f(\mathbf{Y}|\boldsymbol{\theta})]$—namely a matrix of numerical second derivatives of $\log[f(\mathbf{Y}|\boldsymbol{\theta})]$ with respective to the parameters. IC measures such as the AIC (Akaike, 1973) and BIC (Schwarz, 1978) can also be computed using $\log[f(\mathbf{Y}|\boldsymbol{\theta})]$ as (see p. 80, Harvey, 2001):

$$
\begin{aligned}
\mathbf{AIC} &= -2\log[f(\mathbf{Y}|\boldsymbol{\theta})] + 2q \\
\mathbf{BIC} &= -2\log[f(\mathbf{Y}|\boldsymbol{\theta})] + q \log\left(\sum_{i}^{n} T_i\right),
\end{aligned}
$$

where q is the number of parameters in a model.

As explained in Kim & Nelson (1999), the collapsing procedure only yields an approximation of $\hat{\boldsymbol{\eta}}_i(t_{i,j}|t_{i,j})^m$ and $\mathbf{P}_i(t_{i,j}|t_{i,j})^m$ due to the averaging of distant regime history beyond $t_{i,j-1}$ (i.e., $t_{i,1}, \ldots, t_{i,j-2}$). Thus, because of the truncation errors in the collapsing procedure and also the truncation of higher-order terms in the Taylor series expansion that resulted in the ODEs in (8)–(9),

optimizing the log-likelihood function in (10) results only in "approximate" maximum likelihood (ML) as opposed to ML estimates.

Step 4. Smoothing. In the social and behavioral sciences, the entire time series of observations has often been collected prior to model fitting, thus negating the need to perform real-time filtering. In such cases, one can refine the latent variable estimates for $\eta_i(t_{i,j})$ and the probability of the unobserved regime indicator, $S_i(t_{i,j})$, based on all the observed information in the sample, yielding the smoothed latent variable estimates, $\hat{\eta}_i(t_{i,j}|T_i) = E(\eta_i(t_{i,j})|\mathbf{Y}_i(T_i))$, and the smoothed regime probabilities, $\Pr[S_i(t_{i,j}) = m|\mathbf{Y}_i(T_i)]$.

Overall, aside from the use of the CDEKF in step 1 to accommodate a continuous-time dynamic process at the latent level coupled with a discrete-time measurement model, Steps 2–4 of the proposed CDEKimF algorithm are identical to those described in Chow & Zhang (2013) and are described in detail in the Supplementary Material section. Further, for diagnostic purposes, it may be of interest to further collapse the conditional estimates of the current regime m to yield the elements labeled as "optional" in Table 1, including $\hat{\eta}_i(t_{i,j}|t_{i,j})$, $\mathbf{P}_i(t_{i,j}|t_{i,j})$, $\boldsymbol{v}_i(t_{i,j})$ and $\boldsymbol{V}_i(t_{i,j})$. The proposed estimation procedures have been implemented in the R package, *dynr* (Ou et al., 2016), available for download from the Comprehensive R Archive Network (CRAN).

4. Empirical Illustration Results

The model depicted in Eqs. 1–3 is a theoretically inspired model designed to describe specific patterns of change in mother–infant dynamics during the SSP procedure. It was used as the basis to evaluate the performance of IC measures in our simulation study. For the analysis of our empirical model, we considered several adaptations/extensions of the model. One of them was a one-regime model with dyad- and session-specific random effects in the infant set-point, denoted below as Model 1 (abbreviated as model M1), expressed as:

$$\frac{dMom_{ig}(t)}{dt} = -r_1^{(M1)}Mom_{ig}(t) + \left(a_{120}^{(M1)} + a_{121}^{(M1)}isReunion2_{ig}\right)$$
$$[Infant_{ig}(t) - Mom_{ig}(t)]$$
$$\frac{dInfant_{ig}(t)}{dt} = -r_2^{(M1)}\left[Infant_{ig}(t) - setpoint_{ig}^{(M1)}(t)\right]$$
$$+ \left(a_{210}^{(M1)} + a_{211}^{(M1)}isReunion2_{ig}\right)\left[Mom_{ig}(t) - Infant_{ig}(t)\right]$$
$$\frac{dsetpoint_{ig}^{(M1)}(t)}{dt} = 0, \tag{11}$$

where the superscript $(M1)$ is used to distinguish the parameters unique to this model from parameters that appear in other similar but non-equivalent models adapted from Eq. 1. In this one-regime model, r_1 and r_2 were still constrained to be nonnegative to reflect their role as the dyad members' rates of approaching their respective set-points. However, the mother- and infant-initiated approach rates were allowed to be session-specific (taking on the values of a_{120} and a_{210}, respectively, in the first reunion session; and the values of $a_{120} + a_{121}$ and $a_{210} + a_{211}$, respectively, in the second reunion session). We did not explicitly impose constraints on any of a_{120}, a_{121}, a_{210} and a_{211} because, unlike the two-regime model described earlier, there was no need to concretely define a Proximity-Seeking regime in the one-regime context. In addition, an ODE was added for the set-point parameter to represent this parameter as one of the latent variables, to be handled the same way as $Mom_{ig}(t)$ and $Infant_{ig}(t)$. Person- and session-specific deviations in set-point can be specified in the initial condition structure of the latent variables as:

$$\begin{bmatrix} Mom_{ig}(t_{i,1}) \\ Infant_{ig}(t_{i,1}) \\ setpoint_{ig}(t_{i,1}) \end{bmatrix} \sim N \left(\begin{bmatrix} \bar{y}_{Mom}(t_{i,1}) \\ \bar{y}_{Infant}(t_{i,1}) \\ \mu_{setpoint}^{(M1)} \end{bmatrix}, \mathrm{diag} \begin{bmatrix} \mathrm{Var}\left(y_{Mom}(t_{i,1}) \right) \\ \mathrm{Var}\left(y_{Infant}(t_{i,1}) \right) \\ \sigma_{setpoint}^{2(M1)} \end{bmatrix} \right), \quad (12)$$

where the empirical observed sample means (i.e., $\bar{y}_{Mom}(t_{i,1})$ and $\bar{y}_{Infant}(t_{i,1})$) and variances (i.e., $\mathrm{Var}(y_{Mom}(t_{i,1}))$ and $\mathrm{Var}(y_{Infant}(t_{i,1}))$) of the mother and infant Euclidean measures at the first observed time point were used to set the latent initial means and variances of $Mom_{ig}(t_{i,1})$ and $Infant_{ig}(t_{i,1})$.[3] In contrast, the group and across-session average set-point for the infant, $\mu_{setpoint}^{(M1)}$, and the corresponding random effect variance in set-point, $\sigma_{setpoint}^{2(M1)}$, were specified as parameters to be estimated.

Model M1 was compared to a two-regime model adapted from the model in Eqs. (1)–(3). One of the adaptations we made was motivated by difficulties in estimating all the infant-related set-point parameters due to the relatively brief periods of time most infants stayed at a "set-point" away from the mothers (if at all), particularly in the second reunion session. Many infants' set-points also varied in exact location over time. Thus, in model M2 we omitted the random effect for the infant's set while in the Exploration regime (in which $S_{ig}(t) = 1$) and set the set-point parameter to be invariant across infants. The ODE for the mother in the exploration remains unchanged compared to (1). The ODE equations for the Proximity-Seeking regime (in which $S_{ig}(t) = 1$) were adapted slightly to allow more convenient and straightforward testing of possible between-session deviations in Proximity-Seeking behaviors as:

$$\frac{\mathrm{d}Mom_{ig}(t)}{\mathrm{d}t} = \exp\left(a_{120,2}^{(M2)} + a_{121,2}^{(M2)} isReunion2_{ig} \right) \left[Infant_{ig}(t) - Mom_{ig}(t) \right]$$
$$\frac{\mathrm{d}Infant_{ig}(t)}{\mathrm{d}t} = \exp\left(a_{210,2}^{(M2)} + a_{211,2}^{(M2)} isReunion2_{ig} \right) \left[Mom_{ig}(t) - Infant_{ig}(t) \right], \quad (13)$$

where the incorporation of the exponential constraints ensures that the Proximity-Seeking rates for the mother and the infant, $a_{12,2}^{(M2)} = \exp(a_{120,2}^{(M2)} + a_{121,2}^{(M2)} isReunion2_{ig})$ and $a_{21,2}^{(M2)} = \exp(a_{210,2}^{(M2)} + a_{212,2}^{(M2)} isReunion2_{ig})$, respectively, were nonnegative across both reunion sessions. Note that the same model can also be specified by rewriting the proximity rates in Eq. 13 as $a_{12,2}^{(M2)} = \exp(a_{120,2}^{(M2)}) \exp(a_{121,2}^{(M2)})^{isReunion2_{ig}}$ and $a_{21,2}^{(M2)} = \exp(a_{210,2}^{(M2)}) \exp(a_{211,2}^{(M2)})^{isReunion2_{ig}}$. The linearization procedures built into the general RS-ODE estimation framework allow such nonlinearities and the testing of the hypotheses of $\exp(a_{121,2}^{(M2)}) = 0$ and $\exp(a_{211,2}^{(M2)}) = 0$ to be handled directly using the proposed estimation approach. Such constraints ensure that the Proximity-Seeking rates remain nonnegative for the identifiability reasons detailed earlier. Moreover, doing so results in Proximity-Seeking parameters in the second reunion session that are multiplicative functions of the Proximity-Seeking parameters in the first reunion session.

In total, two models were fit to the empirical data. Although the models used to compare the performance of the IC measures for model selection purposes in a simulation study are simpler adaptations of Models 1–2 to keep the computational costs manageable, we conducted preliminary simulations to verify that the proposed estimation procedures were able to recover the parameters in these models well. In addition, as one possible measure of effect size, we computed a "pseudo"

---

[3]These means and variance parameters could also be estimated as modeling parameters (see, e.g., Chow et al., 2016b). However, because these parameters were not of great substantive interest and with the large numbers of time points within participants in the current data set, slight misspecifications of the values and structures of these specific initial conditions were likely to have minimal impact on the overall estimation. Thus, they were fixed at heuristic, empirically determined values.

R^2 value as:

$$R_q^2 = 1 - \frac{SSe_q}{SSy_q} = 1 - \frac{\sum_{g=1}^2 \sum_{i=1}^n \sum_{j=1}^{T_i} \left[v_{q,ig}(t_{i,j}) \right]}{\sum_{g=1}^2 \sum_{i=1}^n \sum_{j=1}^{T_i} \left[y_{q,ig}(t_{i,j}) - \bar{y}_{q,ig} \right]}, \tag{14}$$

where $v_{q,ig}(t_{i,j}) = y_{q,ig}(t_{i,j}) - \hat{y}_{q,ig}(t_{i,j})$ is the one-step-ahead prediction error defined under Step 1 of the proposed estimation procedures, with $\hat{y}_{q,ig}(t_{i,j})$ being the model-implied true distance from the chair (true score) for the qth member in dyad i in reunion session g at time $t_{i,j}$; $\bar{y}_{q,ig}$ is the mean of that dyad member during session g. Note that this R^2 value is only a crude measure because it could, at times, take on negative values in cases where the sum of squared deviations of the model-implied true scores from the observed data exceeds the corresponding sum of squared deviations based on the observed, person- and session-specific means. Furthermore, computation of $v_{q,ig}(t_{i,j})$ utilizes as the initial condition the filtered estimates of true scores from time $t_{i,j-1}$—namely estimates of latent variable scores derived from a linear combination of model predictions and observed data up to time $t_{i,j-1}$. Thus, the R^2 estimates may overestimate the extent of good fit.

The models considered in this empirical illustration are more complicated than those evaluated in the simulation study. Thus, before proceeding with model comparisons, we performed preliminary simulations to ensure model identifiability and underwent several iterations of fitting Models M1–M2 to the empirical data with different starting values. In addition, we performed targeted sensitivity analysis on the results from fitting Model M2 by imposing minor changes on the initial condition specifications of the model. For instance, we compared the modeling results obtained when the initial LO of the Exploration regime relative to the Proximity-Seeking regime, a_1 (see Eq. 6), was freely estimated as compared to being fixed it at the values of 10, -10 and 1. We noticed that the results with respect to the covariates in the RS functions were sensitive to such modeling changes. However, fixing the process noise variances at a small constant (e.g., we tried 0.01 and 0.0001)—a practice adopted at times in fitting single-regime, deterministic dynamic models (i.e., models with no dynamic noise) to reduce instances of false convergence to local solutions (e.g., Molenaar & Newell, 2003)—led to results that were stable and robust to such minor changes. In contrast, freeing up the process noise variances to be estimated as parameters led to numerical problems in the estimation process. Thus, we fixed the process noise variances at 0.01 in both the one- and two-regime models.

We further observed that the estimated value of $\mu_{setpoint}^{(M2)}$ was sensitive to changes in starting values and boundary constraints imposed during the optimization process. However, estimates involving other parameters remained largely unaltered by changes in the estimated value of $\mu_{setpoint}^{(M2)}$, provided that this value was adequately larger than 0 (i.e., the position of the mother's chair) to adequately distinguish the Exploration regime from the Proximity-Seeking regime. This suggested that this parameter may not be empirically identifiable based on information in this particular data set. Thus, we fixed the value of $\mu_{setpoint}^{(M2)}$ to 6.0 to mirror the largest (rounded) observed distance from the chair across all values of $y_{Infant}(t_{i,j})$ and $y_{Mom}(t_{i,j})$.

Based on the IC measures, the two-regime model (AIC = 19,119.54; BIC = 19,255.13 with 15 parameters; pseudo-R^2 = .95 and .91 for mother and baby, respectively) was preferred over the one-regime model (AIC = 12,7272.75; BIC = 12,7363.15 with 10 parameters; pseudo-R^2 = .81 and .86 for mother and baby, respectively). The estimated error variances for mothers and infants in the two regime-switching models were also smaller and close to zero compared to the estimate from the one-regime model ($\sigma_{e,Mom}^2 = 0.03$ and $\sigma_{e,Infant}^2 = 0.04$ in the two-regime model compared to $\sigma_{e,Mom}^2 = 0.13$ and $\sigma_{e,Infant}^2 = 0.06$ in the one-regime model). Next, we summarize results from model M2 (see the parameter estimates obtained from this model in Table 2), followed by elaborations on potential sources of model misfit.

TABLE 2.
Empirical results from fitting model M2.

Parameters	Descriptions	Estimates (SE)
$r_{1,1}^{(M2)}$	Mother's divergence rate during the Exploration regime	158.72 (0.55)
$r_{2,1}^{(M2)}$	Infant's divergence rate during the Exploration regime	4.08 (0.06)
$setpoint^{(M2)}$	Infant's set-point during the Exploration regime	$= 6.00$
$a_{120,2}^{(M2)}$	Mother's coupling strength to infant during the Proximity-Seeking regime in RE 1	-1.35 (0.05)
$a_{121,2}^{(M2)}$	Deviation in mother's coupling strength to infant during the Proximity-Seeking regime in RE 2 relative to RE 1	-9.21 (33.01)[NS]
$a_{210,2}^{(M2)}$	Infant's coupling strength to mother during the Proximity-Seeking regime in RE 1	-0.81 (0.03)
$a_{211,2}^{(M2)}$	Deviation in infant's coupling strength to mother during the Proximity-Seeking regime in RE 2 relative to RE 1	0.38 (0.04)
$\sigma_{e,Mom}^2$	Mother's measurement error variance	0.03 (0.0002)
$\sigma_{e,Infant}^2$	Infant's measurement error variance	0.04 (0.0003)
a_1	Intercept of initial LO of the Exploration regime	-17.50 (32.31)[NS]
c_1	Intercept of LO of switching from Proximity-Seeking to Exploration regime in RE 1	-2.60 (0.03)
$c_{\Delta,11}$	Deviation in LO of staying within the Exploration regime relative to c_1 in RE 1	3.00 (0.06)
$d_{11,1}$	Effect of meanInfantVocal on LO of staying within the Exploration regime in RE 1	-0.57 (0.15)
$d_{11,2}$	Deviation in LO of staying within the Exploration regime while in RE 2	-0.49 (0.07)
$d_{21,1}$	Effect of meanInfantVocal on LO of switching from Proximity-Seeking to Exploration in RE 1	-1.32 (0.11)
$d_{21,2}$	Deviation in LO of switching from Proximity-Seeking to the Exploration regime while in RE 2	-0.36 (0.04)

Note: RE = reunion session; all parameters, except for those marked with the superscript NS, were estimated to be statistically different from zero. The last subscript, m, after the comma in $r_{1,m}$, $r_{20,m}$, $r_{21,m}$, $a_{120,m}$, $a_{121,m}$, $a_{210,m}$ and $a_{211,m}$ reflects the regime with which these parameters were associated, with $m = 1$ and 2 corresponded to the Exploration regime and Proximity-Seeking regime, respectively.

Results from model fitting (see Table 2) indicated that as distinct from the estimated value of divergence rates for the mothers, the estimated value of divergence rate for the infants was much smaller in magnitude compared to that associated with the mothers ($r_{2,1}^{(M2)} = 4.08$, $SE = 0.06$ for
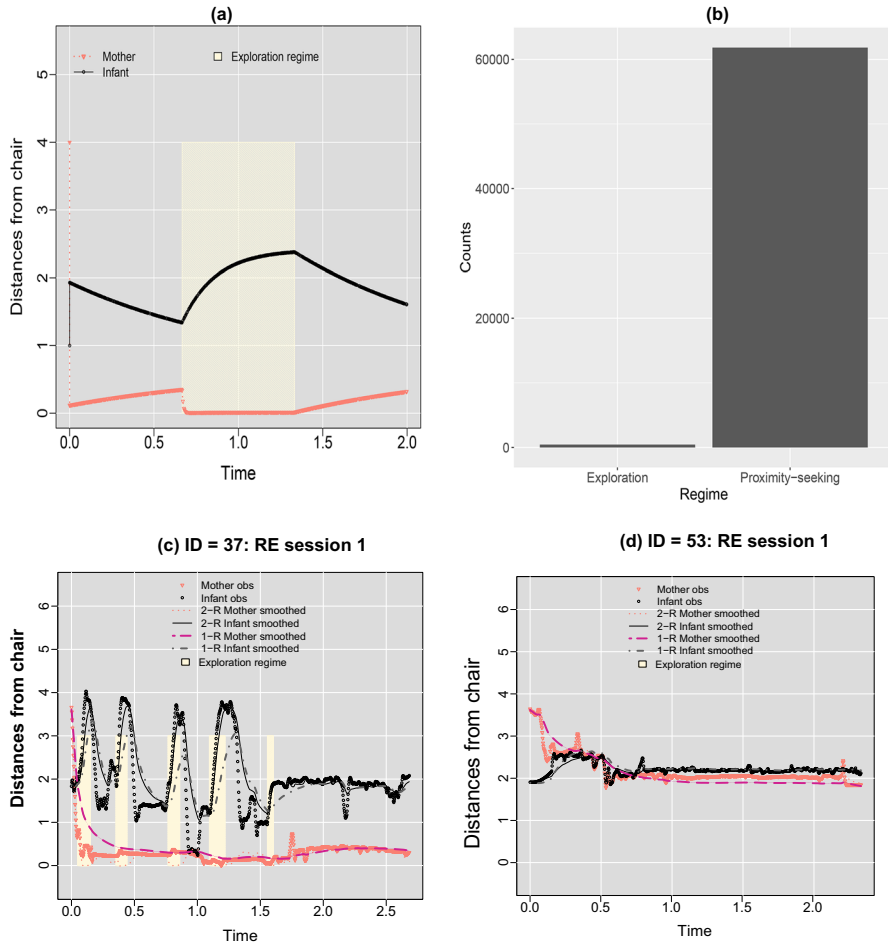
FIGURE 4.

a Simulated trajectories obtained using parameter estimates from empirical model fitting; **b** frequencies of instances across all time points and dyads wherein the two regimes showed higher smoothed regime probabilities than the other regime; **c, d** the observed and smoothed latent variable trajectories obtained from the RS model with covariates and the one-regime model for the two dyads shown in Fig. 3a, b. 2-R = 2-regime model; 1-R = one-regime model.

the infants, as compared to $r_{1,1}^{(M2)} = 158.72, SE = 0.55$ for the mothers). This indicated that infants, even when they were estimated to be in the Exploration regime, were slow in moving away from their mothers. The two members' relative differences in divergence dynamics from each other are shown in the simulated trajectories in Fig. 4a, generated using estimated parameter values from fitting model M2 to data from the second reunion session. In contrast, the infant's Proximity-Seeking strengths were strong in comparison with the mothers' Proximity-Seeking strengths. For instance, in the first reunion session, the Proximity-Seeking strengths for mothers and infants were given, respectively, by $a_{120,2}^{(M2)} = \exp(-1.35) = 0.26$; and $a_{210,2}^{(M2)} = \exp(-0.81) = 0.44$. The Proximity-Seeking strength was found to strengthen for the infants during the second reunion session (as given by $\exp(a_{210,2}^{(M2)} + a_{211,2}^{(M2)}) = \exp(-0.81 + 0.38) = 0.65$ for the infants) but weakened—though not in a statistically reliable way—for the mothers. We set $a_{121,2}^{(M2)}$ to 0 in generating the simulated trajectories in Fig. 4a. These modeling results reflected the distinct changes in the movement dynamics of the infants and mothers with the progress of the SSP

procedure, namely the mothers' desire to instill some autonomy in the infants on the one hand and the infants' growing desire to approach and stay close to their mothers after being separated from them for the second time. Collectively, these parameter estimates yielded relatively abrupt shifts in the predicted movement trajectories of both dyad members, but during different regimes.

The estimated value of $c_{\Delta,11} = 3.00$ (SE $= 0.05$), indicating the deviation in LO of staying within the Exploration regime, when compared to $c_1 = -2.60$ (SE $= 0.03$), the LO of switching from the Proximity-Seeking to the Exploration regime, suggested that in reunion session 1, for infants who did not evidence any vocalizations (i.e., meanInfantVocal$_i$ = isReunion2$_{ig}$ = 0), the probability of staying within the Exploration regime, as given by $\frac{\exp(3.00-2.60)}{\exp(0)+\exp(3.00-2.60)} = .60$, was not very high. Further, with each unit of increase in proportion of infant vocalizations, there was a decrease in the LO for the dyads to stay within the Exploration regime ($d_{11,1} = -0.57$, $SE = 0.15$), as well as a decrease in LO for the dyads to switch from the Proximity-Seeking to the Exploration regime ($d_{21,1} = -1.32$, $SE = 0.11$). There was also a shift in the second reunion session in comparison with the first reunion session toward lower LO of staying within the Exploration regime ($d_{11,2} = -0.49$, $SE = 0.07$) as well as decrease in the LO for the dyads to transition from the Proximity-Seeking to the Exploration regime in the second than in the first reunion session ($d_{21,2} = -0.36$, $SE = 0.04$). These findings suggested that overall infant vocalizations indexed a tendency to maintain Proximity-Seeking, while the second reunion session was associated with simultaneous decline in the desire to transition out of the Proximity-Seeking regime or to stay within the Exploration regime for an extended period of time. Combining all these effects, the overall frequency counts of the more probable regimes across all individuals and time points (based on the highest smoothed regime probability) suggested that the Proximity-Seeking regime was substantially more prevalent than the Exploration regime (see Fig. 4b).

Figure 4c, d shows the predicted (smoothed latent variable) estimates and actual observed data from the two dyads depicted earlier in Fig. 3a, b for reunion session 1. The shaded regions of the plots identify portions of the data where the dyads were predicted to have a higher likelihood of being in the Exploration regime than in the Proximity-Seeking regime (based on $\Pr(S_i(t_{i,j}) = 1|\mathbf{Y}_i(t_{i,j})) \geq .5$). These shaded regions concurred with the measurement occasions on which the members of the dyad were observed to diverge from each other. In particular, dyad 37 was predicted to spend sporadic portions of reunion session 1 in the Exploration regime, whereas the reverse was true for dyad 53. In the same plots, we overlaid the predicted trajectories generated for each of these dyads based on the session-specific one-regime model to help shed light on the ways in which the RS model with covariates was/was not able to enhance the predictions from the one-regime model. Based on the plots, we found that the estimated trajectories from the two-regime model were able to better tailor to differences in the dyads' dynamics while engaging in distinct interactive behaviors, and were able to capture abrupt shifts in dynamics (e.g., in dyad 37 in the first 1.5 minutes during which the infant was observed to show ongoing movements away and toward the mother). In contrast, the one-regime model tended to predict that the dyads settled into and stayed at some set-points that may deviate relatively substantially from the observed locations toward which the dyads settled.

Inspection of the predicted trajectories plotted in Fig. 4c, d revealed several sources of misfit as reflected in the discrepancies between the smoothed latent variable estimates from model M2 and the observed data. One notable discrepancy resided in deviations of the set-point for the mother from 0, due presumably to imprecision either in our estimates of the location of the chair—which could vary slightly from dyad to dyad and even within a session, or some mothers' decision to stay at a set-point away from the chair (e.g., by observing the infant from a distance, but not necessarily from the chair). Based on our post hoc evaluations of the regime classification results, fixing the set-point for all infants arbitrarily at the value of 6.0 led to misclassification of some of the data as being in the Proximity-Seeking regime even though the dyads' dynamics would be

more appropriately classified as being in the Exploration regime. This, in turn, might have led to potential underestimation in the dyads' LO of staying within the Exploration regime. Finally, it is important to note that the two regimes become indistinguishable when $r_{1,1}^{(M2)} = r_{2,1}^{(M2)} = \exp(a_{120,2}^{(M2)} + a_{121,2}^{(M2)}) = \exp(a_{210,2}^{(M2)} + a_{211,2}^{(M2)}) = 0$. This might arise in cases where all mothers and infants stayed exactly at their initial positions and did not show any movements at all. We did not observe this characteristic in this particular data set. That is, most participants did at least show some movements throughout the two reunion sessions; but there were likely reductions in the distinctions between the two regimes with the progress of each reunion session as dyad members settled into specific areas within the room and stopped moving (whether close to, or away from each other). This issue has certainly led to added challenges in isolating the two regimes.

Overall, while the proposed RS-ODE functions offered some improvements over the one-regime models in capturing more abrupt and distinct shifts in dynamics, some unmodeled sources of between- and within-dyad heterogeneities in dynamics did not account for by the group-based ODE and RS functions remained. Some possible modeling extensions that can help circumvent these inadequacies and improve the robustness of these models are highlighted in Discussion section. Despite the potential inadequacies in the dyad-specific regime classification results, the group-based parameter estimates from the RS still help confirm propositions from attachment theory in the preeminent measure of attachment security, the SSP (Ainsworth et al., 1978; Bowlby, 1982), in several important ways. First, they provide overall evidence for interaction with the Strange Situation. Second, they suggest that some children in the SSP vary in time between Proximity-Seeking and Exploration regimes. This is an empirical confirmation of an essential proposition—heretofore lacking in quantitative evidence—first articulated in Bowlby's theory, and given empirical form in Ainsworth's field notes from observing infants and caregivers first in Uganda and then in Baltimore.

Third, they provide evidence that the infant attachment system becomes increasingly activated from the first to the second reunion as evidenced by a decrease in exploration between these Strange Situation episodes and an increase in infant's predilection to stay close to the mother in the second reunion. Fourth, we found that the accumulation of stress due to the separation across reunion sessions did not lead to uniform increase in all aspects of Proximity-Seeking dynamics (as reflected, e.g., in infants' but not mothers' increase in Proximity-Seeking strength from the first to the second reunion session). Although not highlighted in relevant manuals, cross-partner coupling parameters indicate that infants tend to approach their mothers while mothers, following instructions, tend to retreat to their chairs. Finally, they suggest that infant fussy/cry vocalizations function as an attachment behavior or signal, such that infants who exhibit more vocal distress are less likely to transition into or remain in the Exploration regime.

5. Simulation Study

5.1. Simulation Design

The purpose of the simulation study was twofold. We sought to (1) evaluate the performance of the proposed methodological approach in recovering the true values of the parameters and their associated standard error (SE) estimates; and (2) investigate the performance and limitations of model comparison criteria such as the AIC and BIC computed using by-products of the CDEKimF algorithm in detecting model misspecification in RS-DE models. Two configurations of sample size and time series lengths were considered to mirror the sample size of the empirical application, namely with (1) $T_i = 500$ for all i, $n = 40$; and (2) $T_i = 1000$, $n = 20$. The first condition was characterized by fewer observation points than our empirical example but twice the number of dyads; the second condition was similar in sample size configuration to our empirical study. Even

though the corresponding total numbers of time points considered in the two conditions may still be regarded as high by the standards of behavioral sciences, such large-T-small-n configurations are not uncommon with the advent of modern technologies such as smart phones and other mobile devices for collecting ecological momentary assessment data in real time. In addition, the relative differences in aspects of the simulation results can still be contrasted between the two sample size configurations.

The model in Eqs. 1–3 described in Motivating Example section was used as our simulation model. To reduce computational costs, we only considered simulation setup involving a single session and no random effect in the infant set-point parameter. The population values of all the time-invariant parameters were chosen to mirror most of the parameters obtained from empirical model fitting, except that we modified the divergence and approach rates to allow more time for the system to settle into its equilibrium within each regime, and we set the movement metric in terms of centimeters, as opposed to meters as in the empirical example. Specifically, we set the parameters in the dynamic model in Eq. 1 to $r_{1,1} = 0.2$, $r_{2,1} = 0.1$, $a_{12,2} = 0.3$, $a_{21,2} = .2$, $setpoint = 100$, $\sigma^2_{e,Mom} = \sigma^2_{e,Infant} = 9$. We simulated two time-varying covariates to be used in the RS functions. The first covariate, denoted herein as $x_{1i}(t_{i,j})$, was simulated to be a binary covariate which itself has a probability of staying at the values of 0 and 1 of .8 and .8, respectively. The second covariate, denoted herein as $x_{2i}(t_{i,j})$, was set to be a continuous variable following an autoregressive process of order 1 (i.e., an AR(1) process) as $x_{1i}(t_{i,j}) = .9x_{1i}(t_{i,j-1}) + \zeta_{1i}(t_{i,j})$, where $\zeta_{1i}(t_{i,j})$ is normally distributed process noise with mean zero and variance of 0.25.

We assumed that the vector of latent variables at the first time point was normally distributed with means of 70 and 40, and variances of 225 and 100, respectively. We set the initial means and covariance matrix to their true values in the model fitting process. Alternatively, these mean and variances could also be estimated as part of the modeling parameters, but we did not pursue that extension here.

To evaluate the tenability of using AIC and BIC for model comparison purposes in the context of linear RS-DEs, we used these model comparison indices to evaluate the three models considered in our empirical illustration: (1) Model 1, a model with no covariate in the RS function (i.e., $d_{11,1}$, $d_{11,2}$, $d_{21,1}$ and $d_{21,2}$ were all set to 0); (2) Model 2, in which we set the true LO parameters governing the transition between regimes to the values of $c_1 = -4$, $c_{\Delta,11} = 8.5$, $d_{11,1} = -2$, $d_{21,1} = -1$, $d_{11,2} = 1$, and $d_{21,2} = -1$; and (3) Model 3, a one-regime model in which the dynamic parameters were set to the values of $r_{1,1} = 0.2$, $r_{2,1} = 0.1$, $a_{12,2} = 0.3$, $a_{21,2} = .2$, $setpoint = 100$, with other regime-invariant parameters assuming values that were identical to those in Model 1.

In sum, we considered two sample size configurations × three possible data generating models to yield a total of six conditions. Within each of these conditions, all three possible models were fit to each set of generated data and the AIC as well as BIC were calculated. The "best-fitting" model under each model comparison criterion was determined as the model with the lowest AIC and BIC. Five hundred Monte Carlo replications were performed for each condition, and the performance of the AIC and BIC was compared across conditions. In addition, the root mean squared error (RMSE) and relative bias were used to quantify the performance of the approximate ML point estimator only when the correctly specified models were fit to the data. The empirical SE of a parameter (i.e., the standard deviation of the estimates of a particular parameter across all Monte Carlo runs) was used as the "true" standard error. As a measure of the relative performance of the SE estimates, we also included the average relative deviance of a SE (aRDSE) estimate of an estimator, namely the difference between an SE estimate and the true SE over the true SE, averaged across Monte Carlo runs.

Ninety five percent confidence intervals were constructed for each of the Monte Carlo replications in each condition by adding and subtracting 1.96*SE estimate in each replication to the

TABLE 3.
Summary statistics of parameter estimates for model 2, $T = 1000$ and $n = 20$ across 500 Monte Carlo replications.

	True θ	Mean $\hat{\theta}$	RMSE	rBias	SD	$a\widehat{SE}$	Bias SE	aRDSE	Power	95% Coverage
$r_{1,1}$	0.20	0.20	0.000	-0.001	0.001	0.001	0.039	0.000	1.00	0.96
$r_{2,1}$	0.10	0.10	0.000	-0.003	0.001	0.001	-0.014	-0.000	1.00	0.94
$a_{12,2}$	0.30	0.30	0.000	-0.001	0.002	0.002	0.087	0.000	1.00	0.97
$a_{21,2}$	0.20	0.20	0.000	-0.001	0.001	0.002	0.110	0.000	1.00	0.97
$setpoint$	100.00	100.08	0.080	0.001	0.473	0.474	0.003	0.001	1.00	0.95
$\sigma^2_{e,Mom}$	9.00	8.98	0.017	-0.002	0.083	0.091	0.097	0.008	1.00	0.96
$\sigma^2_{e,Child}$	9.00	8.99	0.008	-0.001	0.091	0.090	-0.004	-0.000	1.00	0.95
c_1	-4.00	-4.07	0.070	0.018	0.123	0.120	-0.023	-0.003	1.00	0.92
$c_{\Delta,11}$	8.50	8.66	0.160	0.019	0.254	0.242	-0.048	-0.012	1.00	0.88
$d_{11,1}$	-1.00	-1.03	0.029	0.029	0.243	0.233	-0.039	-0.010	0.97	0.92
$d_{21,1}$	-2.00	-2.11	0.108	0.054	0.454	0.376	-0.172	-0.078	1.00	0.93
$d_{11,2}$	-1.00	-1.00	0.003	0.003	0.085	0.086	0.019	0.002	1.00	0.95
$d_{21,2}$	-1.00	-1.03	0.029	0.029	0.243	0.233	-0.039	-0.010	0.97	0.92

True θ = true value of a parameter; mean $\hat{\theta} = \frac{1}{H} \sum_{h=1}^{H} \hat{\theta}_h$, where $\hat{\theta}_h$ = estimate of θ from the hth MC replication; RMSE $= \sqrt{\frac{1}{H} \sum_{h=1}^{H} (\hat{\theta}_h - true\ \theta)^2}$; RB = relative bias $= \frac{1}{H} \sum_{h}^{H} (\hat{\theta}_h - true\ \theta)/true\ \theta$; SD = standard deviation of $\hat{\theta}$ across Monte Carlo runs; $a\widehat{SE}$ = average standard error estimate across Monte Carlo runs; Bias SE $= a\widehat{SE} - SE$; aRDSE = average relative deviance of $\widehat{SE} = (a\widehat{SE} - SD)/SD$; power = the proportion of 95% confidence intervals (CIs) that do not contain 0 across the MC replications; 95% Coverage = the proportion of 95% confidence intervals (CIs) that contain the true parameter value across the MC replications.

parameter estimate from the replication. The coverage performance of a confidence interval was assessed with its empirical coverage rate, namely the proportion of 95% CIs covering θ across the Monte Carlo replications. Power was computed as the proportion of 95% CIs excluding 0 across the Monte Carlo replications. Finally, we monitored the convergence rates of the different models across sample size conditions by calculating the proportion of convergent Monte Carlo replications.

5.2. Simulation Results

5.2.1. Estimation Quality When Fitting Correctly Specified Models. Statistical properties of the approximate ML estimator across all conditions are summarized in Tables 3 and 4. Due to space constraints, we only present in these tables detailed summary statistics from fitting Model 2—the model with covariates in the RS functions. For comparisons across models and sample size configurations, we plotted the RMSEs and relative biases of the point estimates, aRDSEs of the estimated SEs in comparison with the empirical SEs, 95%coverage rates and convergence rates in Fig. 5a–e, as grouped by the type of parameters, model, and sample size configuration. That is, we averaged the outcome measures within each model and sample size condition as grouped by three types of parameters:(1) dynamic parameters that appear in the ODE functions, including $r_{1,1}, r_{2,1}, a_{12,2}, a_{21,2}$ and $setpoint$; (2) LO parameters that appear in the RS functions, including c_1 to $d_{21,1}$; and (3) measurement error variances in **R**, including $\sigma^2_{e,Mom}$ and $\sigma^2_{e,Infant}$.

In general, when the correctly specified models were fit, the point estimates associated with all the parameters displayed small relative biases across all sample size conditions. RMSEs were

TABLE 4.
Summary statistics of parameter estimates for model 2, $T = 500$ and $n = 40$ across 500 Monte Carlo replications

	True θ	Mean $\hat{\theta}$	RMSE	rBias	SD	$a\widehat{SE}$	Bias SE	aRDSE	Power	95% Coverage
$r_{1,1}$	0.20	0.20	0.000	0.001	0.001	0.001	0.118	0.000	1.00	0.96
$r_{2,1}$	0.10	0.10	0.000	0.001	0.001	0.001	0.050	0.000	1.00	0.96
$a_{12,2}$	0.30	0.30	0.000	0.001	0.002	0.002	0.005	0.000	1.00	0.95
$a_{21,2}$	0.20	0.20	0.000	0.001	0.001	0.001	-0.013	-0.000	1.00	0.94
$setpoint$	100.00	100.03	0.028	0.000	0.254	0.261	0.026	0.007	1.00	0.96
$\sigma^2_{e,Mom}$	9.00	9.00	0.001	-0.000	0.091	0.091	0.002	0.000	1.00	0.95
$\sigma^2_{e,Child}$	9.00	8.99	0.007	-0.001	0.095	0.091	-0.050	-0.005	1.00	0.94
c_1	-4.00	-4.03	0.034	0.008	0.120	0.114	-0.056	-0.007	1.00	0.94
$c_{\Delta,11}$	8.50	8.60	0.098	0.012	0.221	0.204	-0.076	-0.017	1.00	0.91
$d_{11,1}$	-1.00	-1.03	0.031	0.031	0.202	0.184	-0.093	-0.019	1.00	0.92
$d_{21,1}$	-2.00	-2.08	0.083	0.042	0.328	0.294	-0.102	-0.033	1.00	0.94
$d_{11,2}$	-1.00	-0.99	0.005	-0.005	0.083	0.078	-0.062	-0.005	1.00	0.94
$d_{21,2}$	-1.00	-1.03	0.031	0.031	0.202	0.184	-0.093	-0.019	1.00	0.92

True θ = true value of a parameter; mean $\hat{\theta} = \frac{1}{H} \sum_{h=1}^{H} \hat{\theta}_h$, where $\hat{\theta}_h$ = estimate of θ from the hth MC replication; RMSE $= \sqrt{\frac{1}{H} \sum_{h=1}^{H} (\hat{\theta}_h - true\ \theta)^2}$; RB = relative bias $= \frac{1}{H} \sum_h^H (\hat{\theta}_h - true\ \theta)/true\ \theta$; SD = standard deviation of $\hat{\theta}$ across Monte Carlo runs; $a\widehat{SE}$ = average standard error estimate across Monte Carlo runs; Bias SE $= a\widehat{SE} - SE$; aRDSE = average relative deviance of $\widehat{SE} = (a\widehat{SE} - SD)/SD$; Power = the proportion of 95% confidence intervals (CIs) that do not contain 0 across the MC replications; 95% coverage = the proportion of 95% confidence intervals (CIs) that contain the true parameter value across the MC replications.

slightly elevated for the RS-related parameters (see Fig. 5a), due possibly to the truncations of the full regime history in estimating the latent variables and all modeling parameters (see Supplementary Material section). There was a slight tendency for most dynamic (ODE) and RS parameters to show lower RMSEs and relative biases in point estimates in the larger compared to smaller n condition. This finding was largely consistent with previous findings involving similar dynamic models (e.g., discrete-time regime-switching models and ODE models without regime switching; Chow & Zhang, 2013; Chow et al., 2016a; Yang & Chow, 2010), except that previous studies have reported greater improvements in the accuracy and precision of the dynamic parameters with increases in T as opposed to n. Inspection of Tables 3, 4 revealed that the more noticeable differences in RMSE and relative bias in point estimates stemmed primarily from the gain in accuracy as well as precision in estimating the parameter $setpoint$ with larger than smaller n. In addition, inspection of Fig. 5a–b revealed that the quality of the point estimates for the ODE parameters in Model 3 was slightly better with larger T and smaller n, as opposed to smaller T and larger n. This shows that increasing T is instrumental in helping to improve the accuracy of point estimates of ODE parameters in models with more complex dynamic functions. That is, even though Models 1 and 2 were arguably more "complex" (i.e., were characterized by more freely estimated parameters), the ODE functions within each regime were actually simpler in Models 1 and 2 than in Model 3, which required simultaneous estimation of the functionally correlated parameters, $r_{1,1}$–$a_{21,2}$, within the one hypothesized regime. In contrast, increasing n has more notable effects in improving the accuracy of the point estimates of most other parameters, including the RS parameters, the measurement error variance parameters, and selected dynamic parameters, such as $setpoint$.
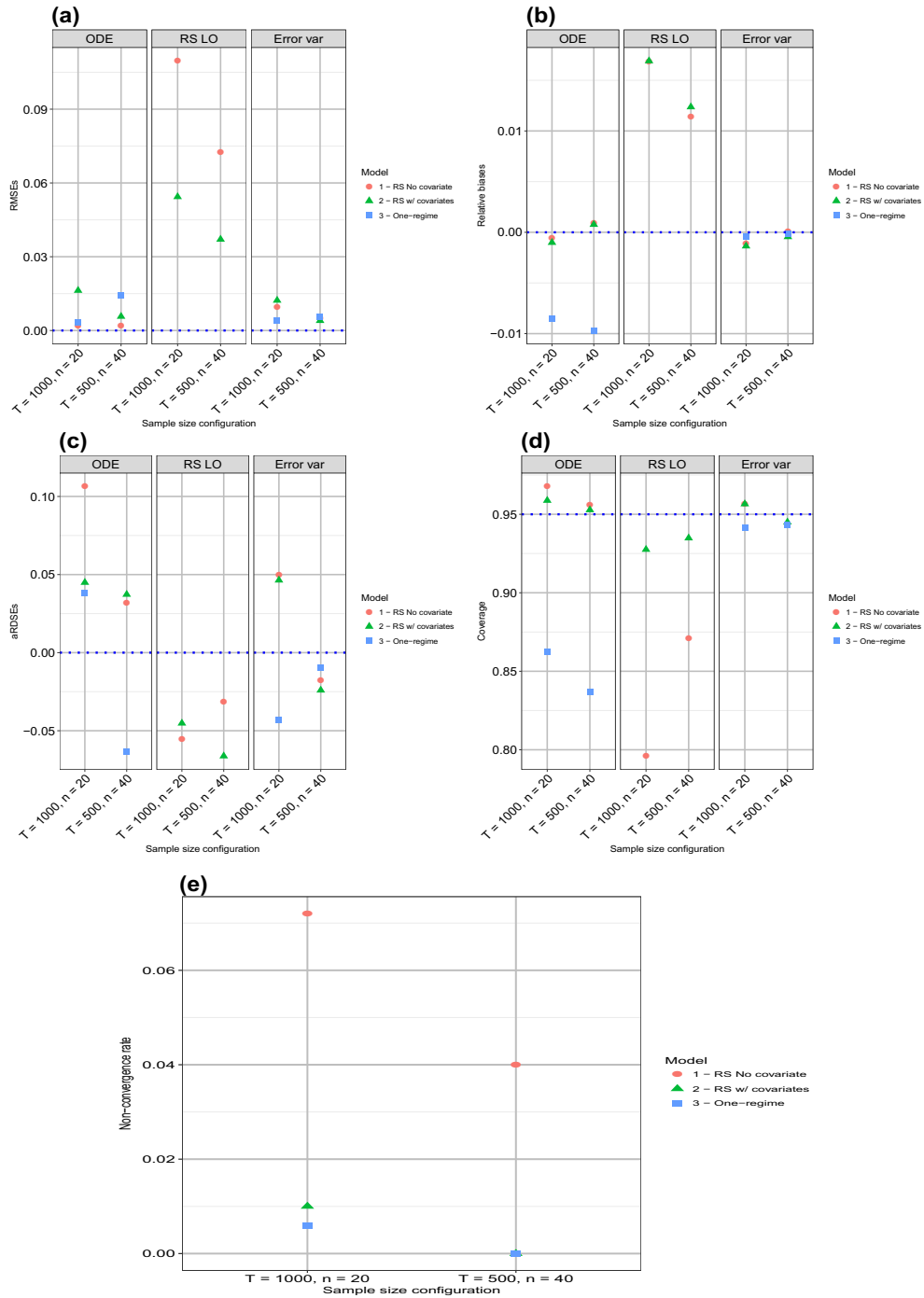
FIGURE 5.
As grouped by model and parameter type, the plots show: **a–b** plots of the average RMSEs and relative biases of the point estimates, **c** relative deviances of the SE estimates (aRDSEs); **d** coverage rates; and **e** convergence rates. ODE = parameters in the ODE functions; RS LO = parameters in the regime-switching functions; error var = measurement error variances.

The sample size condition with larger n and smaller T, compared to the condition with smaller n and larger T, were observed to exhibit slightly greater efficiency (in the sense of smaller average SE estimates and relatedly, smaller true SEs), as well as smaller biases in the SE estimates, particularly in the RS-related parameters, and the parameter *setpoint*. The negative values of RDSE observed for most of the RS-related parameters in Tables 3, 4 suggested that there was a tendency for the SE estimator to underestimate the true variability in these parameters. Figure 5c further clarifies that on average, the underestimation was observed in both Models 1 and 2; slight overestimation in SEs (as evidenced by the positive aRDSEs) was observed for the ODE-related parameters in Models 1 and 2, but not Model 3. Thus, underestimation of SE appeared to be more salient in situations involving more functionally related dynamic parameters with lower T (i.e., in Model 3 and under $T = 500$, but not under $T = 1000$).

The aRDSEs and biases in SE estimates were particularly pronounced in $d_{21,1}$, the regression slope of the binary covariate, $x_{1i}(t_{i,j})$, on the LO of switching from regime 2 (Proximity-Seeking) to regime 1 (Exploration). This parameter was also observed to show large Monte Carlo SD across replications compared to other parameters. The lower precision and efficiency associated with estimating this parameter, particularly in the smaller n condition, may be related to the fact that for a binary covariate, limited information is available to estimate the corresponding shift in transition LO unless a categorical shift in value occurs. In this particular simulation study, the time-varying covariate was generated such that a shift in value occurred probabilistically as governed by a first-order Markov chain process (i.e., with a transition probability matrix that specified the probabilities of the current value of the covariate given its value at the previous time point). Thus, in smaller-n conditions, there may not be enough independent instances of such shifts over time. This was in contrast to larger-n conditions in which information from distinct subjects can be more effectively pooled to improve estimation precision.

For all conditions, when the correctly specified models were fit, the coverage rates of the 95% CIs were relatively close to the .95 nominal rate for most of the modeling parameters. Slightly lower coverage values were observed for some RS parameters (more notably in Model 1 than in Model 2), and the ODE parameters in Model 3 (see Fig. 5d). Overall, coverage rates remained largely similar between the two sample size conditions. Across all models, there was a slight tendency for coverage properties to improve from the smaller-n to the larger-n condition, except in conditions involving Model 3, as consonant with the finding of greater underestimation in SE in this model in the larger-n condition. In addition, due in part to the higher RMSEs observed for the RS-related parameters and the higher aRDSEs for the ODE parameters in the simpler RS model with no covariate (Model 1), the more complex Model 2 with RS-related covariates was found to have slightly better coverage properties than Model 1. Thus, there may be some advantages in including covariates to capture potential regime shifts in the system if good covariates are indeed available.

5.2.2. Model Evaluation Results Using AIC and BIC   Model evaluation results based on the AIC and the BIC are summarized in Table 5, in which we show the proportions of Monte Carlo trials in which the AIC and BIC correctly selected the true model out of the three models considered (Models 1–3), as well as the proportions of convergent trials for which valid log-likelihood values were available at the time of convergence for the computation of the IC measures. Results indicated that out of all the valid trials, the BIC selected the correctly specified model greater than or equal to 93% of the time regardless of whether the true model was Model 1, 2 or 3. Consistent with past findings in the literature, the AIC demonstrated a slight tendency to select overly complex models. Specifically, when the true model was Model 1, the AIC tended to select the overly complex Model 2 as the preferred model a small percentage of the time—a tendency that was slightly more severe in the larger-T than in the smaller-T condition. The AIC still selected the

TABLE 5.
Model evaluation results obtained from the two IC measures considered.

True Model n/T	Model 1 20/1000	Model 2 20/1000	Model 3 20/1000	Model 1 40/500	Model 2 40/500	Model 3 40/500
p(AIC prefers true model)	0.84	0.99	0.99	0.85	1.00	1.00
p(BIC prefers true model)	0.93	0.99	0.99	0.96	1.00	1.00
p(valid cases from Model 1)	0.95	0.48	0.59	0.98	0.65	0.68
p(valid cases from Model 2)	0.96	0.99	0.87	0.97	1.00	0.71
p(valid cases from Model 3)	0.62	0.64	0.99	0.63	0.56	1.00

$p(.)$ indicates the proportion of Monte Carlo replications that demonstrated the property summarized in parentheses. These proportions were calculated from the subset of trials that did pass the convergence criteria of the estimation algorithms.

correct Model 1 greater than or equal to 83% of the time, but with slightly less consistency than the BIC.

One other finding to note was the low number of converged trials from which the IC measures could be computed when mis-specified models were fit to the simulated data. When the correctly specified models were fit, we were able to use close to 100% of the convergent trials for model comparison purposes. When incorrectly specified models were fit, many Monte Carlo trials that had to be excluded due to non-positive definite Hessian and other matrices that require inversion in the estimation process (e.g., the prediction error covariance matrix, $\mathbf{V}_i(t_{i,j})$; see Eq. 10). It was observed, for instance, that when Model 3 was the true data generation model, fitting the highly over-parameterized Model 2 to the corresponding data yielded only 64% and 56% of valid cases for the computation of IC measures in the $T = 1000$ and $T = 500$ conditions, respectively. Despite the general issue of non-convergence when mis-specified models were considered, we found that the AIC and especially the BIC—when they could be computed—selected the correctly specified RS-DE models with high accuracy at the sample sizes considered.

6. Discussion

In the present article, we demonstrated the utility of a special subclass of RS-DE models in representing discrete shifts in dyadic dynamics and make available the estimation algorithms for dealing with these models through the R package, *dynr*. The proposed linear RS-DE model was motivated by an empirical dataset in which infant-mother dyads showed evidence of intermittent transitions between an Exploration and a Proximity-Seeking regime. The dynamics of the dyad members were distinct during different portions or phases of the data; the precise time points at which each dyad may transition between the regimes—if at all—were unknown, but might be explained in part with known covariates or predictors.

Results from our simulation study showed that the proposed estimation procedures performed well under the sample size configurations considered in the present study. The point and SE estimates generally exhibited good accuracy, and the AIC and especially the BIC—when they could be computed—selected the correctly specified RS-DE models with high accuracy at the sample sizes considered. A number of areas are still in need of improvement, however. First, our simulation study was designed to mirror several key features of our empirical data. Thus, our simulation results may be limited in generalizability to other conditions and models of change. Second, we only used the AIC and BIC to evaluate specific aspects of the model (e.g., comparison between variations of the proposed one- and two-regime models). It may be helpful to consider alternative

fit indices and model comparison criteria such as the sample size-adjusted BIC, bootstrap likelihood ratio tests, and other alternative measures (e.g., Nylund et al., 2007; Enders & Tofighi, 2008; Tofghi & Enders, 2007).

Third, we did not consider other more complex models involving more than two regimes, nor did we evaluate the tenability of using these IC measures to compare models with and without random effects. Computational cost was a key consideration. We used an R package, *dynr*, which uses C as the language for the computational backbone while providing an interface in R for model specification. For the simulation study, each Monte Carlo replication for the $T = 1000$ and $n = 20$ condition took approximately 15 minutes of processing time on an Intel(R) Core(TM) i7-4770 3.40 Gigahertz (GHz) Central Processing Unit (CPU) with 8.00 Gigabytes of RAM. However, the computational time increased notably to about 2–3 hours for fitting the more complicated two-regime models in the empirical application because it involved twice as much data within dyads (in terms of time points) as the simulation study. Aside from *dynr*, other statistical programs that can handle matrix operations, such as R (R Development Core Team, 2009), SAS/IML (SAS Institute Inc., 2008), GAUSS (Aptech Systems Inc., 2009), and OxMetrics (Doornik, 1998) may also be used. Other standard structural equation modeling programs such as Mplus (Muthén & Muthén, 2001) and Open-Mx (Boker et al., 2011), the msm (Jackson, 2011) and depmix (Visser, 2007) packages in R, and the PROC LTA procedure in SAS (Lanza & Collins, 2008) can be used to fit hidden Markov models and/or latent transition models. However, these programs currently do not allow for the specification of ODEs, particularly ODEs with regime-switching properties. Future studies should compare the relative performance of different estimation approaches under overlapping subsets of models and also the performance of the CDEKimF under a broader range of models.

Fourth, the mathematical and empirical identifiability (e.g., inability to estimate parameters such as the set-point parameter with high accuracy due to insufficient time spent at the equilibrium) of the modeling parameters is a critical issue that determines the performance of the estimation (Miao et al., 2011). Researchers such as Shapiro (1985, 1986) and Dijkstra (1992) have discussed regularity conditions required for an estimator to show desirable asymptotic properties. The proposed one-regime model satisfies these regularity conditions, but as noted earlier, the two-regime model does have the potential to be located on the boundary of the parameter space (e.g., when both the divergence and Proximity-Seeking rates are at zero), which renders regime separation challenging or even impossible. This is an issue that often arises in the fitting, for instance, of mixture and latent class models. Even if the model is mathematically identifiable, the data may not provide sufficient information to identify the different regimes implicated in the model (e.g., individual differences in the set-point parameter in our empirical application). Although some post hoc diagnostic information (e.g., the positive definiteness of the negative Hessian matrix at the point of convergence) may be gleaned from the estimation process to inform modelers of the presence and severity of this issue, subsequent model refinements and modifications may still prove to be a challenging process.

Fifth, in the present study, we had to impose additional boundary constraints on the dynamic parameters and particular RS parameters to enable the extraction of confirmatory, theoretically meaningful regimes In practice, however, confirmatory constraints motivated by theoretical models may not apply to all dyads' data and inevitably require some modifications when applied to real data. Future work to guide the process of model developments and refinements would be an important contribution to the literature.

Finally, as noted earlier, the collapsing procedure used in the proposed CDEKimF involves an approximation procedure to make the computational process feasible when used with intensive longitudinal data. As a result, the log-likelihood function optimized in the process of fitting the RS-DE models is also an approximation to the exact log-likelihood function used in RS structural equation models involving relatively few numbers of time points (Dolan et al., 2005; Dolan, 2009;

Nylund-Gibson et al., 2013; Schmittmann et al., 2005). This limits, to some extent, the complexity of the RS functions permissible unless, of course, the numbers of time points and individuals are large enough to overcome the approximation errors that arise from the collapsing procedure. The point and SE estimates from the simulation study appeared satisfactorily despite the truncation errors, but this may not be the case in situations involving fewer time points.

Results from our empirical application suggested that some of the subtle differences in dyadic dynamics would likely be bypassed if the data were analyzed as if they conformed to only one single regime. Other modeling alternatives and extensions are, of course, possible. For instance, we found through post hoc evaluations that the mothers' set-points actually deviated to various degrees from 0—our estimated location of their set-point based on the location of the chair in the experimental room. A preferred approach may be to estimate the mothers' individualized set-points as random effects in the models. In addition, rather than allowing the divergence rates and coupling strengths of the dyad members to show discrete shifts contingent on differences between regimes, it may be possible to use ODE/SDE functions or other dynamic models with time-varying parameters (e.g., Chow et al., 2011) to detect and represent other possible patterns of change in these parameters. Formalizing how the proposed ODE models may be extended as SDEs with freely estimated process noise variances (e.g., Oud & Jansen, 2000; Oravecz et al., 2009; Voelkle et al., 2012) is another natural extension. Frequentist extensions that accommodate categorical and non-normal data would also be an important extension (Fahrmeir and Tutz, 2001).

We incorporated limited, very targeted forms of nonlinearities into model M2 in our empirical example to ensure that the Proximity-Seeking parameters were nonnegative across both dyad members and reunion sessions. One interesting extension is to allow the divergence rates and coupling strengths of the dyad members to depend on the dynamics of the other dyad members to further capitalize on the ability of the proposed CDEKimF algorithm to handle nonlinear DE models. Another extension includes allowing the current regime indicator, $S_i(t_{i,j})$, to not only depend on the regime at a previous time point, namely $S_i(t_{i,j-1})$, but also on other earlier regimes. The latter extension is motivated by the general framework implemented in SEM-based programs such as Mplus (Muthén & Asparouhov, 2011) and it extends the transition probability model from a first-order Markov process to higher-order Markov processes. The feasibility of adopting higher-order Markov specifications in a DE modeling framework with the use of the collapsing procedures is yet to be investigated, however.

Other extensions to the work presented in the current study may be considered. Sensitivity of the modeling results to parameter starting values, initial condition specification, choices of ODE solvers, integration time steps, and model complexity are all important issues that warrant further attention. In addition, we assumed that all individuals were characterized by the same set of ODE functions. This assumption may not be tenable in other applications (Molenaar, 2004). Our general modeling and estimation framework can still be used with single-subject data in cases involving adequate number of time points from each individual. In our preliminary simulations, we found that the estimation results were greatly improved and much more stable within the context of the proposed model—particularly among the RS-related LO parameters— if information was pooled across $n \geq 10$ subjects. Beyond the group-based solution utilized in this study, mixed effects variations of the proposed models (Oravecz et al., 2009; Lu et al., 2015) and alternative formulations that combine features of exploratory procedures for identifying idiosyncratic individual deviations from a group-based confirmatory model may be other viable alternatives (e.g., Gates & Molenaar, 2012).

Appendix

Sample *dynr* Code

The R package, *dynr*, can be downloaded from CRAN. Here, we include some sample codes for fitting the empirically motivated model in Eqs. 1–3 to simulated data.

```r
rm(list=ls())
require(dynr)


thedata = read.table('Model2simData.txt',
col.names=c("ID","deltaT","DV1","DV2","cov1","cov2"))

# ---- Model with covariates in RS functions ----

data2 <- dynr.data(thedata, id="ID", time="deltaT",
                   observed=c("DV1","DV2"),
                   covariates=c("cov1", "cov2"))


# Measurement model
meas <- prep.measurement(
  values.load=diag(c(1,1)), #Matrix of factor loading values
  # Diagonal elements are fixed at the values shown in
  #values.load
  params.load = diag(c("fixed","fixed"),2),
  obs.names = c("DV1","DV2"), #Labels for observed variables
  state.names=c('Mom','Infant')) #Labels for latent variables

mean0 = c(70,40)
var0 = c(225,100)

# Initial conditions on the latent variales:means,covariance and
#initial probability structures (if applicable)
initial <- prep.initial(
  values.inistate=mean0,
  params.inistate=c("fixed", "fixed"),
  values.inicov=diag(var0),
  params.inicov=diag("fixed",2),
  values.regimep=c(1, 0),
  params.regimep=c("fixed", "fixed")
)

#Specify ODE formula
formula=list(
  list(Mom~ -r1 * Mom,
       Infant~ -r2*(Infant-base1)),
  list(Mom~  a12 * (Infant - Mom),
       Infant~  a21 * (Mom - Infant)))
```

```
dynm<-prep.formulaDynamics(formula=formula,
                           startval=c(r1=.1,r2=.1,
                           a12=.1,a21=.1, base1 = 95),
                           isContinuousTime=TRUE)


#Regime-switching functions
regimes <- prep.regimes(
  values=matrix(c(6,-1.5,-1,rep(0,3),
                  -3,.5,-.3,rep(0,3)),
               nrow=2, ncol=6,byrow=T),
  # nrow=numRegimes, ncol=numRegimes*(numCovariates+1)
  params=matrix(c("a_11","d_111","d_112",rep("fixed",3),
                  "a_21","d_211","d_212",rep("fixed",3)),
               nrow=2, ncol=6,byrow=T), covariates
               =c("cov1","cov2"),deviation=TRUE)

#measurement and dynamic noise covariance structures
mdcov <- prep.noise(
  values.latent=diag(0, 2),
  params.latent=diag(c("fixed","fixed"), 2),
  values.observed=diag(c(10,10)),
  params.observed=diag(c("sigmasq_e1","sigmasq_e2"),2))

#Impose additional parameter constraints
#Constraining the r1 and r2 parameters to be positive by
imposing the exponential
#transformation functions (through formula.trans).
  The reverse transformation,
#formula.inv, also needs to be provided.
trans<-prep.tfun(formula.trans=list(r1~exp(r1),
                                    r2~exp(r2)),
                 formula.inv=list(r1~log(r1),
                                  r2~log(r2)))

#Put together all the model recipes and data
model2R.2cov <- dynr.model(dynamics=dynm, measurement=meas,
noise=mdcov, initial=initial,
regimes=regimes, transform=trans,
data=data2,outfile="temp2.c")

#Impose some upper and lower parameter boundary constraints
model2R.2cov$ub=c(rep(exp(1.5), 4), 200, exp(5), exp(5),
                  rep(30, 6))
model2R.2cov$lb=c(rep(exp(-20), 4), 50, exp(-10), exp(-10),
                  rep(-30, 6))
```

```
#Cook it!
res2R.2cov <- dynr.cook(model2R.2cov)
summary(res2R.2cov)

#Check model by printing out LaTeX code
printex(model2R.2cov,ParameterAs= model2R.2cov$param.names,
        printInit = TRUE, printRS=TRUE,outFile="RSLinearODE.tex")

#Compare to true parameter values
truePar = c(.2, .1, .3, .2 ,100,9,9,8.5,-4,1,-1,-1,-2)

#Extract other useful information
coef(res2R.2cov)
AIC(res2R.2cov); BIC(res2R.2cov)

#Some plotting functions available as part of dynr
p1 = dynr.ggplot(res2R.2cov, dynrModel=model2R.2cov,
                 names.regime=c("Exploration",
                                "Proximity-Seeking"),
                 names.state=c("Mom","Infant"),
                 title="Results from final RS-linear ODE model",
                 numSubjDemo=2,
                 text=element_text(size=14),style=2)
print(p1)
plot(res2R.2cov,dynrModel=model2R.2cov)
```

References

Ainsworth, M. D. S., Blehar, M. C., Waters, E., & Wall, S. (1978). *Patterns of attachment: A psychological study of the strange situation*. Oxford: Lawrence Erlbaum.

Akaike, H. (1973). Information theory and an extension of the maximum likelihood principle. In B. N. Petrov & F. Csaki (Eds.), *Second international symposium on information theory* (pp. 267–281). Budapest: Akademiai Kiado.

Aptech Systems Inc. (2009). *GAUSS (Version 10)*. WA: Black Diamond.

Arnold, L. (1974). *Stochastic differential equations*. New York: Wiley.

Bar-Shalom, Y., Li, X. R., & Kirubarajan, T. (2001). *Estimation with applications to tracking and navigation: Theory algorithms and software*. New York: Wiley.

Behrens, K. Y., Parker, A. C., & Haltigan, J. D. (2011). Maternal sensitivity assessed during the strange situation procedure predicts child's attachment quality and reunion behaviors. *Infant Behavior and Development*, *34*(2), 378–381.

Beskos, A., Papaspiliopoulos, O., & Roberts, G. (2009). Monte carlo maximum likelihood estimation for discretely observed diffusion processes. *The Annals of Statistics*, *37*(1), 223–245.

Boker, S. M., Deboeck, P. R., Edler, C., & Keel, P. K. (2010). Generalized local linear approximation of derivatives from time series. In S. Chow, E. Ferrer, & F. Hsieh (Eds.), *Statistical methods for modeling human dynamics: An interdisciplinary dialogue* (pp. 161–178). New York: Taylor & Francis.

Boker, S. M., & Graham, J. (1998). A dynamical systems analysis of adolescent substance abuse. *Multivariate Behavioral Research*, *33*, 479–507.

Boker, S. M., Neale, H., Maes, H., Wilde, M., Spiegel, M., Brick, T., et al. (2011). Openmx: An open source extended structural equation modeling framework. *Psychometrika*, *76*(2), 306–317.

Boker, S. M., Neale, M. C., & Rausch, J. (2008). Latent differential equation modeling with multivariate multi-occasion indicators. In K. van Montfort, H. Oud, & A. Satorra (Eds.), *Recent developments on structural equation models: Theory and applications* (pp. 151–174). Amsterdam: Kluwer.

Bolger, N., Davis, A., & Rafaeli, E. (2003). Diary methods: Capturing life as it is lived. *Annual Review of Psychology*, *54*, 579–616.

Bowlby, J. (1973). *Separation: Anxiety & anger. Attachment and Loss. (International psycho-analytical library no. 95)* (Vol. 2). London: Hogarth Press.

Bowlby, J. (1982). *Attachment* (2nd ed., Vol. 1). New York: Basic Books.

Casella, G., & Berger, R. L. (2001). *Statistical inference* (2nd ed.). Pacific Grove: Duxbury Press.

Chow, S.-M., Bendezú, J. J., Cole, P. M., & Ram, N. (2016a). A comparison of two- stage approaches for fitting nonlinear ordinary differential equation (ode) models with mixed effects. *Multivariate Behavioral Research*, *51*(2–3), 154–184.

Chow, S.-M., Ferrer, E., & Nesselroade, J. R. (2007). An unscented kalman filter approach to the estimation of nonlinear dynamical systems models. *Multivariate Behavioral Research*, *42*(2), 283–321.

Chow, S.-M., Ho, M.-H. R., Hamaker, E. J., & Dolan, C. V. (2010). Equivalences and differences between structural equation and state-space modeling frameworks. *Structural Equation Modeling*, *17*, 303–332.

Chow, S.-M., Lu, Z., Sherwood, A., & Zhu, H. (2016b). Fitting nonlinear ordinary differential equation models with random effects and unknown initial conditions using the stochastic approximation expectation maximization (SAEM) algorithm. *Psychometrika*, *81*, 102–134.

Chow, S.-M., & Zhang, G. (2013). Nonlinear regime-switching state-space (RSSS) models. *Psychometrika: Application Reviews and Case Studies*, *78*(4), 740–768.

Chow, S.-M., Zu, J., Shifren, K., & Zhang, G. (2011). Dynamic factor analysis models with time-varying parameters. *Multivariate Behavioral Research*, *46*(2), 303–339.

Collins, L. M., & Wugalter, S. E. (1992). Latent class models for stage-sequential dynamic latent variables. *Multivariate Behavioral Research*, *28*, 131–157.

Deboeck, P. R. (2010). Estimating dynamical systems: Derivative estimation hints from Sir Ronald A Fisher. *Multivariate Behavioral Research*, *45*, 725–745.

Dijkstra, T. K. (1992). On statistical inference with parameter estimates on the boundary of the parameter space. *British Journal of Mathematical and Statistical Psychology*, *45*(2), 289–309.

Dolan, C. V. (2009). Structural equation mixture modeling. In R. E. Millsap & A. Maydeu-Olivares (Eds.), *The SAGE handbook of quantitative methods in psychology* (pp. 568–592). Thousand Oaks: Sage.

Dolan, C. V., & Molenaar, P. C. M. (1991). A note on the calculation of latent trajectories in the quasi Markov simplex model by means of regression method and the discrete kalman filter. *Kwantitatieve Methoden*, *38*, 29–44.

Dolan, C. V., Schmittmann, V. D., Lubke, G. H., & Neale, M. C. (2005). Regime switching in the latent growth curve mixture model. *Structural Equation Modeling*, *12*(1), 94–119.

Doornik, J. A. (1998). *Object-oriented matrix programming using Ox 2.0*. London: Timberlake Consultants Press.

Durbin, J., & Koopman, S. J. (2001). *Time series analysis by state space methods*. New York: Oxford University Press.

Elliott, R. J., Aggoun, L., & Moore, J. (1995). *Hidden markov models: Estimation and control*. New York: Springer.

Enders, C., & Tofighi, D. (2008). The impact of misspecifying class-specific residual variances in growth mixture models. *Structural Equation Modeling: A Multidisciplinary Journal*, *15*, 75–95.

Fahrmeir, L., & Tutz, G. (2001). *Multivariate statistical modelling based on generalized linear models*. Berlin: Springer.

Fukuda, K., & Ishihara, K. (1997). Development of human sleep and wakefulness rhythm during the first six months of life: Discontinuous changes at the 7th and 12th week after birth. *Biological Rhythm Research*, *28*, 94–103.

Gates, K. M., & Molenaar, P. C. M. (2012). Group search algorithm recovers effective connectivity maps for individuals in homogeneous and heterogeneous samples. *Neuroimage*, *63*, 310–319.

Hamilton, J. D. (1989). A new approach to the economic analysis of nonstationary time series and the business cycle. *Econometrica*, *57*, 357–384.

Harvey, A. C. (2001). *Forecasting, structural time series models and the Kalman filter*. Cambridge: Cambridge University Press.

Jackson, C. H. (2011). Multi-state models for panel data: The msm package for R. *Journal of Statistical Software*, *38*(8), 1–29.

Jazwinski, A. H. (1970). *Stochastic processes and filtering theory*. New York: Academic Press.

Jones, R. H. (1993). *Longitudinal data with serial correlation: A state-space approach*. Boca Raton: Chapman & Hall/CRC.

Kalman, R. E., & Bucy, R. S. (1961). New results in linear filtering and prediction theory. In *Trans. ASME, Ser. D, J. Basic Eng,* p 109.

Kim, C.-J., & Nelson, C. R. (1999). *State-space models with regime switching: Classical and Gibbs-sampling approaches with applications*. Cambridge: MIT Press.

Kulikov, G., & Kulikova, M. (2014). Accurate numerical implementation of the continuous-discrete extended Kalman filter. *IEEE Transactions on Automatic Control*, *59*(1), 273–279.

Kulikova, M. V., & Kulikov, G. Y. (2014). Adaptive ODE solvers in extended Kalman filtering algorithms. *Journal of Computational and Applied Mathematics*, *262*, 205–216.

Lanza, S. T., & Collins, L. M. (2008). A new SAS procedure for latent transition analysis: Transitions in dating and sexual risk behavior. *Developmental Psychology*, *44*(2), 446–456.

Lawley, D. N., & Maxwell, M. A. (1971). *Factor analysis as a statistical method* (2nd ed.). London: Butterworths.

Lu, Z.-H., Chow, S.-M., Sherwood, A., & Zhu, H. (2015). Bayesian analysis of ambulatory cardiovascular dynamics with application to irregularly spaced sparse data. *Annals of Applied Statistics*, *9*, 1601–1620.

Mbalawata, I. S., Särkkä, S., & Haario, H. (2013). Parameter estimation in stochastic differential equations with markov chain monte carlo and non-linear Kalman filtering. *Computational Statistics*, *28*(3), 1195–1223.

Miao, H., Xin, X., Perelson, A. S., & Wu, H. (2011). On identifiability of nonlinear ODE models and applications in viral dynamics. *SIAM Review*, *53*(1), 3–39.

Molenaar, P. C. M. (2004). A manifesto on psychology as idiographic science: Bringing the person back into scientific psychology-this time forever. *Measurement: Interdisciplinary Research and Perspectives*, *2*, 201–218.

Molenaar, P. C. M., & Newell, K. M. (2003). Direct fit of a theoretical model of phase transition in oscillatory finger motions. *British Journal of Mathematical and Statistical Psychology*, *56*, 199–214.

Muthén, B. O., & Asparouhov, T. (2011). *LTA in Mplus: Transition probabilities influenced by covariates*. Mplus web notes: No. 13. Available at http://www.statmodel.com/examples/LTAwebnote.pdf. Accessed 23 July 2016.

Muthén, L. K., & Muthén, B. O. (2001). *Mplus: The comprehensive modeling program for applied researchers: User's guide (1998–2001)*. Los Angeles: Muthén & Muthén.

Nylund, K. L., Asparouhov, T., & Muthén, B. O. (2007). Deciding on the number of classes in latent class analysis and growth mixture modeling: A Monte Carlo simulation study. *Structural Equation Modeling*, *14*(4), 535–569.

Nylund-Gibson, K., Muthén, B. O., Nishina, A., Bellmore, A., & Graham, S. (2013). Stability and instability of peer victimization during middle school: Using latent transition analysis with covariates, distal outcomes, and modeling extensions. *Manuscript submitted for publication*.

Oravecz, Z., Tuerlinckx, F., & Vandekerckhove, J. (2009). A hierarchical Ornstein-Uhlenbeck model for continuous repeated measurement data. *Psychometrika*, *74*, 395–418.

Oravecz, Z., Tuerlinckx, F., & Vandekerckhove, J. (2011). A hierarchical latent stochastic differential equation model for affective dynamics. *Psychological Methods*, *16*, 468–490.

Ou, L., Hunter, M. D., & Chow, S.-M. (2016). *dynr: Dynamic Modeling in R*. R package version 0.1.7-22.

Oud, J. H. L., & Jansen, R. A. R. G. (2000). Continuous time state space modeling of panel data by means of SEM. *Psychometrika*, *65*(2), 199–215.

Oud, J. H. L., & Singer, H., (Eds.) (2008). *Special issue: Continuous time modeling of panel data*, Vol. 62.

Oud, J. H. L., van den Bercken, J. H., & Essers, R. J. (1990). Longitudinal factor score estimation using the Kalman filter. *Applied psychological measurement*, *14*, 395–418.

Piaget, J., & Inhelder, B. (1969). *The psychology of the child*. New York: Basic Books.

Pincus, S., Gladstone, I., & Ehrenkranz, R. (1991). A regularity statistic for medical data analysis. *Journal of Clinical Monitoring*, *7*, 335–345.

Press, W. H., Teukolsky, S. A., Vetterling, W. T., & Flannery, B. P. (2002). *Numerical recipes in C*. Cambridge: Cambridge University Press.

R Development Core Team (2009). *R: A language and environment for statistical computing*. Vienna: Austria. ISBN: 3-900051-07-0.

Ramsay, J. O., Hooker, G., Campbell, D., & Cao, J. (2007). Parameter estimation for differential equations: a generalized smoothing approach (with discussion). *Journal of Royal Statistical Society: Series B*, *69*(5), 741–796.

Särkkä, S. (2013). *Bayesian Filtering and Smoothing*. Hillsdale: Cambridge University Press.

SAS Institute Inc. (2008). *SAS 9.2 help and documentation*. Cary, NC.

Schmittmann, V. D., Dolan, C. V., van der Maas, H., & Neale, M. C. (2005). Discrete latent Markov models for normally distributed response data. *Multivariate Behavioral Research*, *40*(2), 207–233.

Schwartz, J. E., & Stone, A. A. (1998). Strategies for analyzing ecological momentary assessment data. *Health Psychology*, *17*, 6–16.

Schwarz, G. (1978). Estimating the dimension of a model. *The Annals of Statistics*, *6*, 461–464.

Schweppe, F. (1965). Evaluation of likelihood functions for Gaussian signals. *IEEE Transactions on Information Theory*, *11*, 61–70.

Shapiro, A. (1985). Asymptotic distribution of test statistics in the analysis of moment structures under inequality constraints. *Biometrics*, *72*(1), 133–44.

Shapiro, A. (1986). Asymptotic theory or overparameterized structural models. *American Statistical Association Journal*, *81*(393), 142–149.

Sherwood, A., Thurston, R., Steffen, P., Blumenthal, J. A., Waugh, R. A., & Hinderliter, A. L. (2001). Blunted nighttime blood pressure dipping in postmenopausal women. *American Journal of Hypertension*, *14*, 749–754.

Singer, H. (2002). Parameter estimation of nonlinear stochastic differential equations: Simulated maximum likelihood vs. extended Kaman filter and itô-Taylor expansion. *Journal of Computational and Graphical Statistics*, *11*, 972–995.

Singer, H. (2003). Nonlinear continuous discrete filtering using kernel density estimates and functional integrals. *Journal of Mathematical Sociology*, *27*, 1–28.

Singer, H. (2010). Sem modeling with singular moment matrices part i: Ml-estimation of time series. *The Journal of Mathematical Sociology*, *34*(4), 301–320.

Singer, H. (2012). Sem modeling with singular moment matrices part ii: Ml-estimation of sampled stochastic differential equations. *The Journal of Mathematical Sociology*, *36*(1), 22–43.

Sivalingam, R., Cherian, A., Fasching, J., Walczak, N., Bird, N., Morellas, V., Murphy, B., Cullen, K., Lim, K., Sapiro, G., & Papanikolopoulos, N. (2012). A multi-sensor visual tracking system for behavior monitoring of at-risk children. In *IEEE international conference on robotics and automation (ICRA)*.

Tofghi, D., & Enders, C. K. (2007). Identifying the correct number of classes in mixture models. In G. R. Hancock & K. M. Samulelsen (Eds.), *Advances in latent variable mixture models* (pp. 317–341). Greenwich: Information Age.

Trail, J. B., Collins, L. M., Rivera, D. E., Li, R., Piper, M. E., & Baker, T. B. (2013). Functional data analysis for dynamical system identification of behavioral processes. *Psychological Methods*, *19*, 175–182.

van der Maas, H. L. J., & Molenaar, P. C. M. (1992). Stagewise cognitive development: An application of catastrophe theory. *Psychological Review*, *99*(3), 395–417.

Van Geert, P. (2000). The dynamics of general developmental mechanisms: From Piaget and Vygotsky to dynamic systems models. *Current Directions in Psychological Science*, *9*(2), 64–68.

Vecchiato, W. (1997). New models for irregularly spaced time series analysis with applications to high frequency financial data. In *Proceedings of the IEEE/IAFE 1997 computational intelligence for financial engineering (CIFEr)*, pp. 144–149.

Visser, I. (2007). *Depmix: An R-package for fitting mixture models on mixed multivariate data with markov dependencies*. Technical report, University of Amsterdam.

Voelkle, M. C., Oud, J. H. L., Davidov, E., & Schmidt, P. (2012). An sem approach to continuous time modeling of panel data: relating authoritarianism and anomia. *Psychological Methods*, *17*, 176–192.

Waters, E. (2002). Comments on strange situation classification. Retrieved on May 1, 2012 from http://www.johnbowlby.com.

Yang, M., & Chow, S.-M. (2010). Using state-space model with regime switching to represent the dynamics of facial electromyography (EMG) data. *Psychometrika: Application and Case Studies*, *74*(4), 744–771.